

Incentivizing Federated Learning under Long-Term Energy Constraint via Online Randomized Auctions

Yulan Yuan, Lei Jiao, *Member, IEEE*, Konglin Zhu, *Member, IEEE*, and Lin Zhang, *Member, IEEE*

Abstract—Mobile users are often reluctant to participate in federated learning to train models, due to the excessive consumption of the limited resources such as the mobile devices’ energy. We propose an auction-based online incentive mechanism, FLORA, which allows users to submit bids dynamically and repetitively and compensates such bids subject to each user’s long-term battery capacity. We formulate a nonlinear mixed-integer program to capture the social cost minimization in the federated learning system. Then we design multiple polynomial-time online algorithms, including a fractional online algorithm and a randomized rounding algorithm to select winning bids and control training accuracy, as well as a payment allocation algorithm to calculate the remuneration based on the bid-winning probabilities. Maintaining the satisfiable quality of the global model that is trained, our approach works on the fly without relying on the unknown future inputs, and achieves provably a sublinear regret and a sublinear fit over time while attaining the economic properties of truthfulness and individual rationality in expectation. Extensive trace-driven evaluations have confirmed the practical superiority of FLORA over existing alternatives.

I. INTRODUCTION

FEDERATED learning [1], [2] is a novel distributed machine learning paradigm that allows mobile devices (e.g., smart phones, vehicular computing platforms [3], [4]) to hold raw training data on premises, train the target model locally, and only communicate the model update to a logically centralized server (e.g., a cloud or edge data center) for aggregation in an iterative manner. Unlike conventional distributed machine learning, federated learning has the core benefit of protecting user’s privacy since no raw data need to be uploaded to the server [5], [6], and receives increasing interests in the forthcoming era of 5G, Internet of Things, and Artificial Intelligence. However, mobile users are often reluctant to participate in federated learning due to the excessive resource consumption [7], [8], especially given the limited battery

Manuscript received May 8, 2021; revised September 16, 2021; accepted December 6, 2021. This work was supported in part by the Hunan Province Science and Technology Project Funds 2018TP1036, in part by the Key Laboratory of Modern Measurement & Control Technology, Ministry of Education, Beijing Information Science & Technology University KF20211123202, and in part by the U.S. National Science Foundation under Grant CNS-2047719. (Corresponding authors: Konglin Zhu; Lei Jiao.)

Y. Yuan and L. Zhang are with the School of Artificial Intelligence, Beijing University of Posts and Telecommunications, Beijing, China (e-mail: {yuanyl, zhanglin}@bupt.edu.cn).

L. Jiao is with the Department of Computer and Information Science, University of Oregon, Eugene, OR 97403, USA (e-mail: jiao@cs.uoregon.edu).

K. Zhu is with the School of Artificial Intelligence, Beijing University of Posts and Telecommunications, Beijing, China and Purple Mountain Laboratories, Nanjing, China (e-mail: klzhu@bupt.edu.cn).

Color versions of one or more figures in this article are available online at xxx.

Digital Object Identifier xxx.

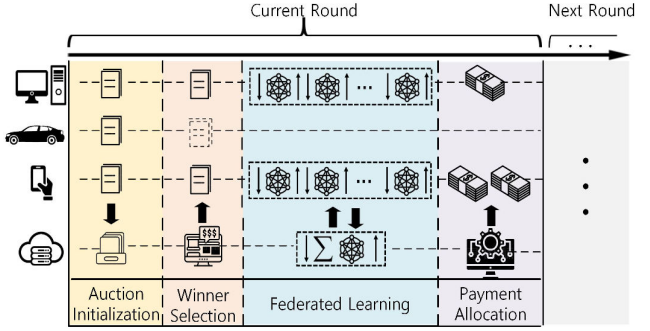


Fig. 1: Auction model for federated learning

energy of today’s mobile devices, which motivates the need of designing a mechanism to incentivize users’ participation [9], [10]. “Auction” can be an approach to fulfill this goal, i.e., letting the server be the auctioneer and conduct multiple rounds of auctions to select and purchase the bids offered by the mobile devices which can be the bidders. The server thus performs federated learning with the winning bids and makes the corresponding payments. Compared to an alternative of letting the mobile devices directly pricing their data, the auction approach is agile to dynamic markets and can better reflect the real-time demand-supply [11].

Unfortunately, designing an appropriate auction mechanism for federated learning is never an easy task, and faces multiple fundamental challenges as follows.

- **Challenge 1: Long-term constrained online setting.**

The mechanism is intrinsically not a static one-time transaction [6], but needs to handle repetitive auctions on the fly subject to each mobile device’s long-term battery capacity. Each mobile device may generate a varying amount of raw training data and offer different bids as time elapses [2], [12]. If some bids are selected currently and the corresponding devices consume battery to execute federated learning (shown in Fig. 1), then such devices may not be able to be selected again in the future even when they have more training data, due to insufficient battery. As the server and each mobile device often have no knowledge about the future inputs, such as training data volumes and network conditions, it is nontrivial to decide the winning bids in an online manner.

- **Challenge 2: Intractability.** Pursuing resource efficiency of the mobile devices should not be at the cost of sacrificing the quality of the model being trained and delivered in the federated learning process [6]. The total resource consumption, including the computation and communication energy and the bandwidth for calculating

and transferring the model updates [7], [10], [13], often relates nonlinearly to the quality of the model in terms of the total loss over all the training data. Intertwined with bid selection, the problem can often be NP-hard, making it difficult to control the system and to strike the balance between model training and resource consumption, especially with heterogeneous mobile devices.

- **Challenge 3: Economic properties.** Our auction mechanism is also expected to achieve the desired economic properties of truthfulness and individual rationality. The former means no bid can achieve a higher utility by cheating on the bidding price and the latter means every bid achieves a non-negative utility, where the utility of a bid refers to the difference between the received payment and the bidding price (i.e., asking price). Conventionally, Vickrey-Clarke-Groves (VCG) mechanisms or their fractional variants can achieve such properties, but they are inapplicable here. VCG requires to solve the underlying problem optimally, yet our problem is intractable [11]; fractional VCG, which is often jointly used with a primal-dual algorithm, is hampered by the long-term constraint and the nonlinearity of our problem.

Existing studies cannot address the aforementioned challenges. There exists a substantial body of work on optimizing federated learning systems in terms of various performance objectives including energy, convergence rate, and communication rounds [1], [6], [14]–[18], but they are not for incentivization, which marks an essential difference. Yet, those few that are on federated learning incentives still fall insufficient, as they are either from contract or game theoretic perspectives [4], [9], [19] with a different focus, or adopt auctions but only consider one-time scenarios and overlook quality of the models being trained [10], [20], not to mention the dynamic online setting and the long-term constraints which escalate the difficulty fundamentally for the mechanism design.

In this paper, we formulate the online optimization problem of minimizing the long-term social cost of all involved parties in the federated learning system as a nonlinear mixed-integer program. Our formulation controls the total resource consumption and the quality of the global model being trained through selecting bids and adjusting the convergence parameter of the loss over the local training data. Enforcing no assumption on how the dynamic inputs may vary over time, our problem captures transmission power, wireless channel gain, dynamic training data volume [1], [16], etc, while conforming to the long-term energy constraint of every single bidder.

We propose a novel mechanism, which we name **FLORA** (**F**ederated **L**earning **O**nline **R**andomized **A**uctions), for incentivizing the mobile devices via auctions and selecting the appropriate bids to participate in federated learning by solving the underlying social cost minimization problem. To this end, we design three polynomial-time algorithms. First, we relax the problem to the real domain and overcome the long-term constraints by designing an alternating ascent-descent online algorithm through reformulating the problem via Lagrange multipliers and introducing a carefully-designed regularization term [21], [22], which does not rely on future inputs. Next, we design a randomized rounding algorithm [23] to convert

fractional solutions from our relaxed problem into integers by rounding pairs of fractions in opposite directions for compensation, without violating instantaneous constraints. Finally, we design the payment allocation algorithm which uses fractional decisions as bid-winning probabilities and composes payments in each auction via the marginal cost of the bidding prices.

We rigorously prove the performance guarantees of our proposed algorithms. We show that our fractional online algorithm and randomized rounding algorithm jointly lead to a sublinear “regret” [22], [24], i.e., the time-average difference between the long-term social cost incurred by our online approach with no knowledge of future inputs and that of the offline optimum with full knowledge of all the inputs will vanish as time elapses, and a sublinear “fit” [25], i.e., the time-average violation of the long-term constraints will also vanish gradually. We show that our payment allocation achieves truthfulness and individual rationality by satisfying the corresponding sufficient and necessary conditions for randomized auctions.

We evaluate the practical performance of our approach extensively, via training Multi-Layer Perception (MLP), Convolutional Neural Network (CNN), and Multinomial Logistic Regression (MLR) models with real-world datasets and federated learning settings. We find the results in multiple aspects, including the following: (1) Achieving the same target convergence of the global model, **FLORA** performs significantly better than other bid-selection methods such as **Random_FL**, **Fixed_FL** and **Greedy_FL**, saving up to 38.9%, 29.0% and 42.1% social cost on average, respectively, and is close to the performance of the **Offline** optimum; (2) **FLORA** achieves truthfulness and individual rationality for every single auction, with the regret and the fit growing very slowly in the long run; (3) **FLORA** produces machine learning models with satisfiable inference accuracy and loss across different training tasks; (4) **FLORA** always uses a smaller number of global iterations for federated learning, consuming moderate training time.

The rest of this paper is structured as follows. Section II summarizes the related literatures and points out how this paper is different and advantageous. Section III presents system models, problem formulation, algorithmic challenges, and an overview of proposed mechanism. Section IV designs a fractional online algorithm and a randomized rounding algorithm for winning-bid selections, and theoretically analyzes the dynamic regret and the dynamic fit. Section V presents the payment allocation algorithm and analyzes the truthfulness and the individual rationality. Section VI conducts trace-driven experiments to evaluate our approach and compares it to multiple alternatives. Section VII concludes the paper.

II. RELATED WORK

We categorize and discuss related work in different groups, and then point out how our work differs from each group.

Optimization of Federated Learning Systems: Yang et. al. [1] designed an iterative algorithm to optimize federated learning over wireless networks while considering energy-efficient transmission and computation. Wang et. al. [2] and Nguyen et. al. [15] studied federated learning in edge computing systems with limited computation and communication resources. Mills

TABLE I: Comparison of existing work on federated learning incentives to this work

Reference	Mechanism	Problem	Online / Offline	Optimization Objective	Constraints	Performance Guarantees
[26]	Stackelberg Game	Convex, nonlinear	Offline	Utility maximization (energy and communication)	Instantaneous	Nash Equilibrium
[9]	Stackelberg Game	Mixed-boolean	Offline	Utility maximization (model quality in local and global accuracy, communication, and computation)	Instantaneous	Nash Equilibrium
[27]	Stackelberg Game	Quasi-concave	Offline	Social welfare maximization (model quality in data size and accuracy, communication, and computation)	Instantaneous	Nash Equilibrium
[28]	Contract Theory	Non-convex, nonlinear	Offline	Social cost minimization (model quality in accuracy loss, energy, and time)	Instantaneous	Individual Rationality
[19]	Contract Theory	Non-convex, nonlinear	Offline	Utility maximization (model quality in local and global accuracy, and energy)	Instantaneous	Incentive Compatibility Individual Rationality
[4]	Contract Theory	Non-convex, nonlinear	Offline	Utility maximization (loss decay, global loss, communication time)	Instantaneous	Incentive Compatibility Individual Rationality
[10]	Auction	Mixed integer, linear	Offline	Social welfare maximization (model quality in local and global accuracy, communication, and computation)	Instantaneous	Truthfulness Individual Rationality
[20]	Auction	Combinatorial, linear	Offline	Social welfare maximization (model quality in weights divergence, communication, and computation)	Instantaneous	Truthfulness Individual Rationality
[12]	Auction	Quasi-concave	Offline	Utility maximization (model quality in data size and data category, and resource quality)	Instantaneous	Nash Equilibrium
This work	Auction	Mixed integer, nonlinear	Online	Social cost minimization (model quality in global and local accuracy, communication, and computation)	Long-term Instantaneous	Truthfulness Individual Rationality

et. al. [29] proposed the communication-efficient FedAvg approach based on ADAM optimization for reducing the number of rounds to convergence. Zhou et. al. [30] designed a cost-efficient optimization framework to coordinate the edge and the cloud for reducing both computation and communication cost. Wang et. al. [31] proposed a communication-mitigated federated learning approach which mitigated the communication overhead. Li et. al. [32] designed a multi-layer online coordination framework for high-performance energy-efficient federated learning. Dinh et. al. [33] proposed a federated learning algorithm which can capture the trade-off between the convergence time and the energy consumption with heterogeneous computing and power resources. Liu et. al. [34] studied adaptive power allocation with the aim of minimizing the learning optimality gap under privacy and power constraints. Prakash et. al. [35] injected structured coding redundancy into federated learning for mitigating stragglers and speeding up the training procedure. Jin et. al. [6] selected participant devices to optimize resource consumption of federated learning. Lu et. al. [3] combined deep reinforcement learning with federated learning to build a hybrid blockchain architecture.

Incentive Mechanisms for Federated Learning: Kang et. al. [19] adopted the contract theory to incentivize mobile devices to support federated learning. Ye et. al. [4] facilitated the interactions between the server and the vehicular clients by employing the two-dimensional contract theory. Shashi et. al. [9] formulated a two-stage Stackelberg game to tackle the utility maximization problem for guaranteeing the communication efficiency. Zeng et. al. [12] designed an incentive mechanism to encourage edge nodes with high quality but low cost to participate in federated learning. Jiao et. al. [20] designed an auction mechanism for the trading between the federated learning platform and the data owners. T. H. T. Le et. al. [10] proposed an auction mechanism for the base station and the

mobile users to collaboratively train models. Feng et. al. [26] used the Stackelberg game approach to investigate the interactions among the mobile devices and the model owner. Ding et. al. [28] considered a multi-dimensional contract-theoretic approach for summarizing users' multi-dimensional private information into a one-dimensional criterion and minimizing the cost of the server. Zhan et. al. [27] proposed a novel incentive mechanism based on Stackelberg games for federated learning in IoT applications.

Our research in this paper differs from both of the above two groups of research. Those [1], [3], [14], [15], [29], [33], [35] that focus on optimizing the federated learning systems in wireless networks, edge computing environments, and vehicular or other platforms largely investigate the problems from an offline perspective, and cannot actually be directly adapted to address the online setting with provable performance guarantees as in our work characterized by unpredictable time-varying inputs and long-term constraints.

Some works [2], [6], [30]–[32], [34] have taken into account the dynamic system and the unpredictable information, but have not approached the problem from the incentive perspective. Regarding the incentive mechanism design for federated learning, some [9], [26], [27] adopt the game-theoretic approach but are not able to provide any guarantee for truthfulness or individual rationality as in our work. Others [4], [19], [28] adopt the contract theory and prove incentive rationality, but they lack the consideration of the long-term energy constraints of the mobile devices, which fundamentally changes the nature of the problem.

They [4], [9], [10], [20] often only consider static one-time transactions, without long-term effects, or consider repetitive auctions [12] but focus on Nash equilibrium instead of economic properties, different from our work in essence. For the optimization objectives, they [4], [26] focus on the energy

TABLE II: NOTATIONS

Input	Description
$\theta_i^{(t)}, \varepsilon_g^{(t)}$	Local accuracy of device i and global accuracy at the time slot t
$D_i^{(t)}$	Set of data samples of device i at the time slot t
$Kl^{(t)}, Kg^{(t)}$	Number of local iterations and global iterations at the time slot t
$w^{(t)}$	Global model trained at the time slot t
$F^{(t)}(\cdot)$	Loss of all participants at the time slot t
$F_i^{(t)}(\cdot)$	Loss of device i and all participants at the time slot t
$\mathbb{E}m_i^{(t)}$	Communication energy consumed per global iteration
$\mathbb{E}p_i^{(t)}$	Computation energy consumed per global iteration
$c_i^{(t)}$	Bidding price of bidder i at the time slot t
Ω_i	Energy limit of device i for auctions
Decision	Description
$x_i^{(t)}$	Whether device i wins the auction at the time slot t
$\delta^{(t)}$	Maximum local accuracy at the time slot t

and communication and lack the assurance of the model quality. To sum up, none of the existing research, to the best of our knowledge, have studied federated learning incentives from an online perspective with guaranteed model quality and provable truthfulness and individual rationality under long-term constraints.

III. MODEL AND PROBLEM FORMULATION

In this section, we present system models, problem formulation, algorithmic challenges and an overview of our proposed mechanism. We summarize the major notations in Table II.

A. System Modeling

Server, Mobile Devices, and Training Data: We consider a system that consists of a federated learning server and a set of mobile devices, represented as $\mathcal{I} = \{1, 2, \dots, I\}$, which can communicate with the server via (cellular) wireless networks. Considering that the system is dynamic, we study it over a series of time slots $\mathcal{T} = \{1, 2, \dots, T\}$. Each mobile device i is equipped with built-in sensors, storage, and a processor for participating in federated learning, powered by the local battery. At the time slot $t \in \mathcal{T}$, every device $i \in \mathcal{I}$ has a collection of data samples $D_i^{(t)}$. A data sample $n \in D_i^{(t)}$ is $\{x_n, y_n\}$, where x_n refers to the features with corresponding values and y_n refers to the ground-truth label.

Federated Learning: Federated learning contains multiple “global iterations”, where each global iteration further consists of the “local training” followed by the “global aggregation”. To train the global model $w^{(t)}$ at the time slot t , we minimize the total loss at t . We define the loss at the mobile device i as $F_i^{(t)}(w^{(t)}) = \frac{\sum_{n \in D_i^{(t)}} f_n^{(t)}(w^{(t)})}{|D_i^{(t)}|}$, where $f_n^{(t)}(w^{(t)})$ is the loss incurred by the single data sample n (calculated based on comparing its ground-truth label to the inferred label produced by $w^{(t)}$ using its feature values), and define the total loss as $F^{(t)}(w^{(t)}) = \sum_{i \in W^{(t)}} \left\{ \frac{|D_i^{(t)}|}{\sum_{i \in W^{(t)}} |D_i^{(t)}|} F_i^{(t)}(w^{(t)}) \right\}$ [10], where $W^{(t)} \subseteq \mathcal{I}$ denotes the set of all the participating mobile devices at t . To solve the problem $\min_{w^{(t)}} F^{(t)}(w^{(t)})$ in an iterative manner, we adopt the federated learning algorithm [13], [15] exhibited below.

We explain the above algorithm further. At the time slot t , in the k -th global iteration, the device i seeks the optimal solution, i.e., $w_{i,k}^{(t)} = \operatorname{argmin}_w J_{i,k}^{(t)}(w|w_{k-1}^{(t)}, \nabla F^{(t)}(w_{k-1}^{(t)}))$, by

Federated Learning Algorithm, $\forall t$

initialize $w_0^{(t)}$ and $\nabla F^{(t)}(w_0^{(t)})$; \triangleright Initialization on server
for $k = 1, \dots, Kg$ do
\triangleright Local training on each device $i \in W^{(t)}$:
download $w_{k-1}^{(t)}$ and $\nabla F^{(t)}(w_{k-1}^{(t)})$ from server;
for $k_2 = 1, \dots, Kl$ do
$w_{i,k,k_2}^{(t)} = w_{i,k,k_2-1}^{(t)} - v \nabla J_{i,k}^{(t)}(w_{i,k,k_2-1}^{(t)})$;
upload $w_{i,k}^{(t)} = w_{i,k,Kl}^{(t)}$ and $\nabla F_i^{(t)}(w_{i,k}^{(t)})$ to server;
\triangleright Global aggregation on server:
$w_k^{(t)} = \frac{1}{ W^{(t)} } \sum_{i \in W^{(t)}} w_{i,k}^{(t)}$
$\nabla F^{(t)}(w_k^{(t)}) = \frac{1}{ W^{(t)} } \sum_{i \in W^{(t)}} \nabla F_i^{(t)}(w_{i,k}^{(t)})$.

executing the gradient-based process of $w_{i,k,k_2}^{(t)} = w_{i,k,k_2-1}^{(t)} - v \nabla J_{i,k}^{(t)}(w_{i,k,k_2-1}^{(t)})$. Here, v is a constant step size, $w_{i,k,0}^{(t)} = w_{k-1}^{(t)}$, and $J_{i,k}^{(t)}(w)$ is a dedicated function defined as $J_{i,k}^{(t)}(w) = F_i^{(t)}(w) - [\nabla F_i^{(t)}(w_{k-1}^{(t)}) - \beta_1 \nabla F^{(t)}(w_{k-1}^{(t)})]^\top (w - w_{k-1}^{(t)}) + \frac{\beta_2}{2} \|w - w_{k-1}^{(t)}\|^2$ [15], where $\beta_1, \beta_2 \geq 0$ are parameters. The problem $\operatorname{argmin}_w J_{i,k}^{(t)}(w|w_{k-1}^{(t)}, \nabla F^{(t)}(w_{k-1}^{(t)}))$ is solved in Kl iterations locally on the device i to achieve a $\theta_i^{(t)}$ -approximation solution $w_{i,k,Kl}^{(t)}$ satisfying $\|\nabla J_{i,k}^{(t)}(w_{i,k,Kl}^{(t)})\| \leq \theta_i^{(t)} \|\nabla J_{i,k}^{(t)}(w_{k-1}^{(t)})\|$, where $\theta_i^{(t)} \in (0, 1)$ is a parameter that can be called “local accuracy”. To make this inequality hold, we need to conduct the following number of local iterations, where \mathcal{V} is a constant [1]:

$$Kl(\theta_i^{(t)}) = \mathcal{V} \log_2 \left(\frac{1}{\theta_i^{(t)}} \right).$$

After Kg global iterations, the global model aggregated on the server is $w_{Kg}^{(t)}$. We would desire $F^{(t)}(w_{Kg}^{(t)}) - F^{(t)}(w^{(t)\star}) \leq \varepsilon_g^{(t)} (F^{(t)}(w_0^{(t)}) - F^{(t)}(w^{(t)\star}))$, where $w^{(t)\star}$ is the optimal solution to the problem $\min_{w^{(t)}} F^{(t)}(w^{(t)})$ and $\varepsilon_g^{(t)} \in (0, 1)$ is a parameter that can be called “global accuracy”. To make this inequality hold, we conduct the following number of global iterations [15]:

$$Kg(\delta^{(t)}) = \frac{\mathcal{O}(\log(1/\varepsilon_g^{(t)}))}{1 - \delta^{(t)}},$$

where $\delta^{(t)} = \max_{i \in \mathcal{W}^{(t)}} \{\theta_i^{(t)}\}$ is the maximum local accuracy across all the participating devices.

Auction: The server, as the auctioneer, conducts an auction at every time slot t in the following four steps as shown in Fig. 1. First, the server solicits bids, and each device i , as the bidder, submits a bid in the format of $\{c_i^{(t)}, \mathcal{B}_i^{(t)}\}$. While $c_i^{(t)}$ refers to the “bidding price”, i.e., the price the bid would want to charge, $\mathcal{B}_i^{(t)}$ contains a set of information: the preferred local accuracy $\theta_i^{(t)}$, the size of the local raw data $|D_i^{(t)}|$ as aforementioned, $\mathbb{E}p_i^{(t)}$, i.e., the computation energy consumed per global iteration, and $\mathbb{E}m_i^{(t)}$, i.e., the communication energy consumed per global iteration. Second, receiving all the bids, the server then determines the winning bids by solving the social cost minimization problem via our proposed algorithm. Third, the server performs the actual federated learning process with the devices corresponding to the selected bids. Fourth, after federated learning finishes,

the server calculates and makes payments to the participant devices through our proposed algorithm. In this paper, to continuously benefit from the auctions in the long run, each device i is also required to submit the “battery capacity” Ω_i to the server. Note that Ω_i is specified by the user, which is no greater than the real amount of the remaining battery energy, and is the amount of energy that the device i is willing to devote at maximum to the federated learning tasks.

We emphasize that conducting such an auction for incentivizing federated learning always keeps the private data $D_i^{(t)}$ at local device i , which adheres the principle of federated learning. However, it is inevitable to exchange other data during the whole process [10]. Consider the information $\{c_i^{(t)}, \mathcal{B}_i^{(t)}\}$ transferred in the auction, we adopt the technique of sealed-bid auction, indicating that only the auctioneer and device i knows this bid [12]. There are related technologies, such as differential privacy [34], which can enhance the privacy protection by introducing noise into data, but this is beyond the scope of this research.

Decision Variables: We focus on making two types of decisions: $x_i^{(t)} \in \{0, 1\}$, indicating whether or not the mobile device i wins the auction and is thus chosen to participate in the federated learning process at the time slot t ; $\delta^{(t)} \in (0, 1)$, indicating the maximum local accuracy across all the participant devices which determines the number of global iterations that need to be performed at the time slot t . Particularly, given the global accuracy $\varepsilon_g^{(t)}$, we control $\delta^{(t)}$ in order to control the cost that is taken to achieve $\varepsilon_g^{(t)}$ for the global model, as elaborated below.

Cost of Mobile Devices: The total cost incurred at the mobile devices at the time slot t is the cost that the bids want to charge, minus any payment received from the server:

$$\sum_t \sum_i x_i^{(t)} (c_i^{(t)} - r_i^{(t)}). \quad (1)$$

During federated learning, each mobile device consumes battery energy for updating the model and also sharing the model with the server. We represent the energy consumption of computation and communication [20] for the mobile device i in each global iteration as

$$\mathbb{E}p_i^{(t)} = K_l^{(t)}(\theta_i^{(t)})\gamma_i|D_i^{(t)}|M$$

and

$$\mathbb{E}m_i^{(t)} = \frac{Mp_i^{(t)}}{B \log_2(1 + \frac{p_i^{(t)}h_i^{(t)}}{N_0B})}$$

respectively, where γ_i is the energy consumption per unit computation in each local iteration; M is the size of the model; $p_i^{(t)}$ is the required transmission power; B is the allocated bandwidth; $h_i^{(t)}$ is the wireless channel gain; and N_0 is the background noise of the wireless channel.

Cost of Server: The total cost incurred at the server at the time slot t contains the computation cost of model aggregation $K_g^{(t)}(\delta^{(t)}) \cdot M \cdot \zeta_1^{(t)}$, where $\zeta_1^{(t)}$ denotes the computation cost per unit size of the model in a single global iteration, and the payment to the bidders $r_i^{(t)}$:

$$\sum_t \sum_i x_i^{(t)} \left(K_g^{(t)}(\delta^{(t)}) \cdot M \cdot \zeta_1^{(t)} + r_i^{(t)} \right). \quad (2)$$

B. Problem Formulation and Algorithmic Challenges

Formulation: We formulate the social cost minimization problem. The “social” cost refers to the total cost of the entire system over the entire time horizon, i.e., the sum of (1) and (2), where the payments are canceled (but still need to be determined based on the solution of the social cost minimization problem, as shown later). Our formulation is

$$\text{Min} \sum_t \sum_i x_i^{(t)} \left(c_i^{(t)} + K_g^{(t)}(\delta^{(t)}) \cdot M \cdot \zeta_1^{(t)} \right) \quad (3)$$

$$\text{s.t. } \sum_t x_i^{(t)} K_g^{(t)}(\delta^{(t)}) (\mathbb{E}p_i^{(t)} + \mathbb{E}m_i^{(t)}) \leq \Omega_i, \forall i \in W^{(t)}, \quad (3a)$$

$$\theta_i^{(t)} x_i^{(t)} \leq \delta^{(t)}, \forall i \in \mathcal{I}, \forall t \in \mathcal{T}, \quad (3b)$$

$$\sum_i x_i^{(t)} |D_i^{(t)}| \geq D^{(t)}, \forall t \in \mathcal{T}. \quad (3c)$$

$$\text{Var. } x_i^{(t)} \in \{0, 1\}, \delta^{(t)} \in (0, 1), \forall i \in \mathcal{I}, \forall t \in \mathcal{T}.$$

The objective (3) minimizes the social cost. Constraint (3a) ensures that the total energy consumption at every mobile device over the entire time horizon respects the battery capacity. Constraint (3b) captures the definition of $\delta^{(t)}$, i.e., the maximum of the local accuracy $\theta_i^{(t)}$, $\forall i$. Constraint (3c) guarantees that sufficient training data are used in the federated learning process at each time slot, where $D^{(t)}$ is a pre-specified threshold on the data volume, which can be designated by the server or system operator based on expected quality of the model to be trained, previous empirical experience, etc.

Challenges: Solving the formulated problem online is non-trivial. First, the long-term constraint, i.e., Constraint (3a), makes a major obstacle. At each time slot, it is hard to determine whether to select a given bid, since selecting a bid and executing federated learning can prematurely run out of the battery of a device so that a better bid which may come from that device in the future cannot be selected. Second, the problem is a nonlinear mixed-integer program and NP-hard (we omit the proof, given that the problem contains an existing NP-hard problem, i.e., the covering problem, as a special case), making it intractable even in the offline setting (i.e., all the inputs over the entire time horizon are revealed in advance), not to mention that we want to solve it in the online setting (i.e., the inputs at a time slot is only revealed as that time slot arrives). Third, we need to determine the payment for each winner and guarantee truthfulness and individual rationality, as defined later, requiring our algorithms to be designed strategically.

C. Overview of the Proposed Mechanism

Our goal is to solve the social cost minimization problem in polynomial time and in an online manner in order to select the winning bids and determine the payments in each auction, and to control and conduct the federated learning process over time. To that end, we propose FLORA demonstrated as Algorithm 1. FLORA invokes Algorithms 2, 3, and 4, where the former two algorithms are described in Section IV and the last one algorithm is described in Section V.

Algorithm 1 is the overall control algorithm and is primarily executed at the federated learning server (except Line 6 which

Algorithm 1: The FLORA Algorithm

```

1 for  $t + 1$ , where  $t = 0, 1, 2, \dots, |\mathcal{T}| - 1$  do
2    $\triangleright$  Winner Selection:
3   Invoke Algorithm 2 to get the fractional solutions;
4   Invoke Algorithm 3 to get the integral solutions;
5    $\triangleright$  Federated Learning:
6   Invoke the Federated Learning Algorithm (Sec. III);
7    $\triangleright$  Payment Allocation:
8   Invoke Algorithm 4 to calculate the payments;

```

is performed at both the server and the mobile devices). Algorithms 2 and 3 are the Online Fractional Algorithm and the Randomized Rounding Algorithm, as in Lines 3 and 4 of Algorithm 1, respectively, jointly determine the winning bids, while overcoming the challenges of the long-term constraint and the intractability. The Online Fractional Algorithm outputs the fractional results which provably guarantee the vanishing time-average violation of the long-term constraint. The Randomized Rounding Algorithm takes the fractional results as inputs and rounds them into integers with provably no violation of other instantaneous constraints. These two algorithms also lead to a vanishing time-average difference between the social cost incurred by our produced online solutions and that incurred by the offline optimum. Algorithm 4 allocates the payment in Line 8, leveraging the randomization and the outputs of Algorithm 3, and can be proven to achieve the properties of both truthfulness and individual rationality.

IV. ONLINE SOCIAL COST MINIMIZATION

For solving our formulated problem, we design an online algorithm to obtain the fractional solutions and then a randomized rounding algorithm to convert the fractional bid-selection decisions to integers. For analyzing the performance of our proposed algorithms, we define two performance metrics, i.e., the dynamic regret and the dynamic fit, and finally we rigorously prove their sublinearity.

A. Online Fractional Algorithm

We relax the bid-selection variables to the real domain and adopt a concise representation for our problem formulation. First, we normalize $\mathcal{O}(\log(1/\varepsilon_g^{(t)}))$ to 1, as the global accuracy $\varepsilon_g^{(t)}$ is a constant at t , so that $Kg(\delta^{(t)}) = \frac{1}{1-\delta^{(t)}}$. We denote the decision variables as $\mathbf{X}^{(t)} = [x_1^{(t)}, \dots, x_I^{(t)}, Kg(\delta^{(t)})]$ ($\delta^{(t)}$ can be derived from $Kg(\delta^{(t)})$, as we solve $Kg(\delta^{(t)})$), and we can express the objective function as $f^{(t)}(\mathbf{X}^{(t)}) = \sum_{i \in \mathcal{I}} x_i^{(t)} (c_i^{(t)} + Kg(\delta^{(t)}) \cdot M \cdot \zeta_i^{(t)})$. We also introduce some new notations: $g_i^{(t)} = x_i^{(t)} Kg(\delta^{(t)}) \mathbb{E}_i^{(t)} - \frac{\Omega_i}{T}$, where $\mathbb{E}_i^{(t)} = \mathbb{E}p_i^{(t)} + \mathbb{E}m_i^{(t)}$; $g_{I+i}^{(t)} = \theta_i^{(t)} x_i^{(t)} Kg(\delta^{(t)}) - Kg(\delta^{(t)}) + 1$, $\forall i \in \{1, \dots, I\}$; $g^{(t)}(\mathbf{X}^{(t)}) = [g_1^{(t)}, \dots, g_I^{(t)}, g_{I+1}^{(t)}, \dots, g_{2I}^{(t)}]^\top$; $h^{(t)}(\mathbf{X}^{(t)}) = \sum_{i \in \mathcal{I}} x_i^{(t)} |D_i^{(t)}| - D^{(t)}$. Then, we reformulate the relaxed problem as follows:

$$\text{Min } \sum_{t \in \mathcal{T}} f^{(t)}(\mathbf{X}^{(t)}) \quad (4)$$

$$\text{s.t. } \sum_{t \in \mathcal{T}} g^{(t)}(\mathbf{X}^{(t)}) \preceq \mathbf{0} \quad (4a)$$

$$h^{(t)}(\mathbf{X}^{(t)}) \geq 0 \quad (4b)$$

$$\text{Var. } \mathbf{X}^{(t)} \in \mathcal{X} = \{\mathbf{X}^{(t)} | x_i^{(t)} \in [0, 1], \forall i; Kg(\delta^{(t)}) > 1\}.$$

Solving the above problem (4) is equivalent to solving its min-max version of the problem, which can be expressed as

$$\begin{aligned} \text{Min}_{\mathbf{X}^{(t)}} \text{Max}_{\boldsymbol{\lambda}^{(t)}} & \sum_t (f^{(t)}(\mathbf{X}^{(t)}) + \boldsymbol{\lambda}^{(t)\top} g^{(t)}(\mathbf{X}^{(t)})) \\ \text{s.t. } & h^{(t)}(\mathbf{X}^{(t)}) \geq 0, \mathbf{X}^{(t)} \in \mathcal{X}. \end{aligned} \quad (5)$$

We denote $\mathcal{L}^{(t)}(\mathbf{X}, \boldsymbol{\lambda}) := f^{(t)}(\mathbf{X}) + \boldsymbol{\lambda}^{(t)\top} g^{(t)}(\mathbf{X})$, where $\boldsymbol{\lambda}^{(t)}$ is the corresponding Lagrange multiplier at t .

We design our online algorithm for the problem (5) now by adopting a standard dual ascent step at $t + 1$ to update the dual variable $\boldsymbol{\lambda}^{(t+1)}$, and a modified descent step to minimize $\mathcal{L}^{(t)}(\mathbf{X}, \boldsymbol{\lambda}^{(t+1)})$ with respect to the primal variable \mathbf{X} . With $\tilde{\mathbf{X}}^{(t)}$, where $\tilde{\mathbf{X}}^{(t)} = [\tilde{x}_1^{(t)}, \dots, \tilde{x}_I^{(t)}, Kg(\delta^{(t)})]$ denotes the (fractional) primal solution solved at t , the dual solution can be calculated as follows at $t + 1$:

$$\boldsymbol{\lambda}^{(t+1)} = [\boldsymbol{\lambda}^{(t)} + \mu g^{(t)}(\tilde{\mathbf{X}}^{(t)})]^+, \quad (6)$$

where μ is the (positive) step size, $g^{(t)}(\tilde{\mathbf{X}}^{(t)}) = \nabla_{\boldsymbol{\lambda}} \mathcal{L}^{(t)}(\tilde{\mathbf{X}}^{(t)}, \boldsymbol{\lambda}^{(t)})$ is the gradient of $\mathcal{L}^{(t)}(\tilde{\mathbf{X}}, \boldsymbol{\lambda})$ given $\boldsymbol{\lambda} = \boldsymbol{\lambda}^{(t)}$. Afterwards, we can obtain the (fractional) primal solution $\tilde{\mathbf{X}}^{(t+1)}$ by solving the following problem at $t + 1$ (note that this problem is in the real domain):

$$\begin{aligned} \text{Min } & \nabla f^{(t)}(\tilde{\mathbf{X}}^{(t)})^\top (\mathbf{X} - \tilde{\mathbf{X}}^{(t)}) + \boldsymbol{\lambda}^{(t+1)\top} g^{(t)}(\mathbf{X}) + \frac{\|\mathbf{X} - \tilde{\mathbf{X}}^{(t)}\|^2}{2\alpha} \\ \text{s.t. } & h^{(t)}(\mathbf{X}) \geq 0, \mathbf{X} \in \tilde{\mathcal{X}}, \end{aligned} \quad (7)$$

where α is a predefined constant and $\nabla f^{(t)}(\tilde{\mathbf{X}}^{(t)})$ is the gradient of $f^{(t)}(\mathbf{X})$ at $\mathbf{X} = \tilde{\mathbf{X}}^{(t)}$. Through such ascent-descent steps, the primal variable and the dual variable, $\mathbf{X}^{(t+1)}$ and $\boldsymbol{\lambda}^{(t+1)}$, can be solved at each time slot $t + 1$ using only the information known so far (and we do not even require $f^{(t+1)}$ when solving for $\tilde{\mathbf{X}}^{(t+1)}$), rather than the unknown future information. We approximate $\mathcal{L}^{(t)}(\mathbf{X}, \boldsymbol{\lambda}^{(t+1)})$ by $\nabla f^{(t)}(\tilde{\mathbf{X}}^{(t)})^\top (\mathbf{X} - \tilde{\mathbf{X}}^{(t)})$ plus $\boldsymbol{\lambda}^{(t+1)\top} g^{(t)}(\mathbf{X})$, and the regularization term $\frac{1}{2\alpha} \|\mathbf{X} - \tilde{\mathbf{X}}^{(t)}\|^2$ is a proximal term. The formulation of the problem (7) is not conventional, which is the key enabler for our performance analysis later. This algorithm is shown as Algorithm 2. Algorithm 2 is polynomial-time, since the problem (7) can be solved using optimization tool which finds the ϵ -accurate optimal solution in $O(I^2 \log(1/\epsilon))$ iterations [36] by the interior point method.

Algorithm 2: Online Fractional Algorithm

Input: Fractional solution $\tilde{\mathbf{X}}^{(t)}$; dual solution $\boldsymbol{\lambda}^{(t)}$

Output: Fractional solution $\tilde{\mathbf{X}}^{(t+1)}$

1 Calculate $\boldsymbol{\lambda}^{(t+1)}$ according to (6);

2 Calculate $\tilde{\mathbf{X}}^{(t+1)}$ by solving the problem (7) optimally.

B. Randomized Rounding Algorithm

We design Algorithm 3 to convert the fractional solutions $[\tilde{x}_1^{(t)}, \dots, \tilde{x}_I^{(t)}]$ from Algorithm 2 into integers $[\bar{x}_1^{(t)}, \dots, \bar{x}_I^{(t)}]$ in a “randomized” manner ($Kg(\delta^{(t)})$ is real and does not need to be rounded), ensuring the following aims: (1) every fraction $\tilde{x}_i^{(t)}$ rounded to an integer $\bar{x}_i^{(t)}$; (2) no violation of constraints after rounding, i.e., $\sum_{i \in \mathcal{I}} \bar{x}_i^{(t)} |D_i^{(t)}| \geq D^{(t)}$; (3)

the expectation preserved after rounding, i.e., $E(\tilde{x}_i^{(t)}) = \tilde{x}_i^{(t)}$. Preserving the expectation is the key to designing randomized auctions. Algorithm 3 is composed of the two components of fractions scaling, which adjusts the current value of every fraction, and fractions rounding, which picks up a pair of fractions in each iteration and rounds them to the opposite directions (i.e., rounding up vs. rounding down) so that their (weighted) sum stays unchanged. We introduce some auxiliary notations: $\tilde{\mathbf{X}}'^{(t)} = [\tilde{x}'_1^{(t)}, \dots, \tilde{x}'_I^{(t)}]$ refers to the intermediate results after fractions scaling; $\tilde{\mathbf{X}}''^{(t)} = [\tilde{x}''_1^{(t)}, \dots, \tilde{x}''_I^{(t)}]$ refers to the intermediate results during fractions rounding.

Algorithm 3: Randomized Rounding Algorithm

Input: Fractions $[\tilde{x}_1^{(t)}, \dots, \tilde{x}_I^{(t)}]$
Output: Integers $[\bar{x}_1^{(t)}, \dots, \bar{x}_I^{(t)}]$

- 1 \triangleright Fractions scaling
- 2 Define $\tilde{\mathbf{W}}^{(t)} = [\tilde{x}_1^{(t)} \cdot |D_1^{(t)}|, \dots, \tilde{x}_I^{(t)} \cdot |D_I^{(t)}|]$,
 $\eta = \mathbf{1}^\top \tilde{\mathbf{W}}^{(t)}$;
- 3 $\omega_1 = \frac{\lceil \eta \rceil}{\eta}, \omega_2 = \frac{\lfloor \eta \rfloor}{\eta}$;
- 4 With probability $\eta - \lfloor \eta \rfloor$, set
 $\tilde{\mathbf{X}}'^{(t)} = [\omega_1 \cdot \tilde{x}_1^{(t)}, \dots, \omega_1 \cdot \tilde{x}_I^{(t)}]$;
- 5 With probability $\lceil \eta \rceil - \eta$, set
 $\tilde{\mathbf{X}}'^{(t)} = [\omega_2 \cdot \tilde{x}_1^{(t)}, \dots, \omega_2 \cdot \tilde{x}_I^{(t)}]$;
- 6 Define $\mathcal{I}' = \mathcal{I} \setminus \{i \mid \tilde{x}'_i \in \{0, 1\}\}$;
- 7 \triangleright Fractions rounding
- 8 **while** $\mathcal{I}' \neq \emptyset$ **do**
- 9 Select $i_1, i_2 \in \mathcal{I}', i_1 \neq i_2$, define $k = \frac{|D_{i_1}^{(t)}|}{|D_{i_2}^{(t)}|}$;
- 10 $\rho_1 = \min\{1 - \tilde{x}'_{i_1}, \frac{1}{k} \tilde{x}'_{i_2}\}$,
 $\rho_2 = \min\{\frac{1}{k} (1 - \tilde{x}'_{i_2}), \tilde{x}'_{i_1}\}$;
- 11 With probability $\frac{\rho_2}{\rho_1 + \rho_2}$,
- 12 set $\tilde{x}''_{i_1} = \tilde{x}'_{i_1} + \rho_1, \tilde{x}''_{i_2} = \tilde{x}'_{i_2} - k\rho_1$;
- 13 With probability $\frac{\rho_1}{\rho_1 + \rho_2}$,
- 14 set $\tilde{x}''_{i_1} = \tilde{x}'_{i_1} - \rho_2, \tilde{x}''_{i_2} = \tilde{x}'_{i_2} + k\rho_2$;
- 15 **if** $\tilde{x}''_{i_1} \in \{0, 1\}$, **then** set
 $\bar{x}_{i_1}^{(t)} = \tilde{x}''_{i_1}, \mathcal{I}' = \mathcal{I}' \setminus \{i_1\}$;
- 16 **else** set $\tilde{x}'_{i_1} = \tilde{x}''_{i_1}$;
- 17 **if** $\tilde{x}''_{i_2} \in \{0, 1\}$, **then** set
 $\bar{x}_{i_2}^{(t)} = \tilde{x}''_{i_2}, \mathcal{I}' = \mathcal{I}' \setminus \{i_2\}$;
- 18 **else** set $\tilde{x}'_{i_2} = \tilde{x}''_{i_2}$;

We explain Algorithm 3 with some details as follows. ω_1 and ω_2 in Line 3 are the amplification factor and the reduction factor, respectively, resulting in either increasing each fraction $\tilde{x}_i^{(t)}$ in Line 4 or decreasing it in Line 5. For Line 4, because of $\tilde{x}'_i^{(t)} \geq \tilde{x}_i^{(t)}$, we have $\sum_{i \in \mathcal{I}} \tilde{x}'_i^{(t)} |D_i^{(t)}| \geq D^{(t)}$. For Line 5, because of $\omega_2 = \frac{\lfloor \eta \rfloor}{\eta}, \sum_{i \in \mathcal{I}} \omega_2 \tilde{x}_i^{(t)} |D_i^{(t)}| = \lfloor \eta \rfloor \geq D^{(t)}$, and $\tilde{x}'_i^{(t)} = \omega_2 \tilde{x}_i^{(t)}$, we have $\sum_{i \in \mathcal{I}} \tilde{x}'_i^{(t)} |D_i^{(t)}| \geq D^{(t)}$. Consequently, we can have $E(\tilde{x}'_i^{(t)}) = (\eta - \lfloor \eta \rfloor) \omega_1 \tilde{x}_i^{(t)} + (\lceil \eta \rceil - \eta) \omega_2 \tilde{x}_i^{(t)} = \lceil \eta \rceil \tilde{x}_i^{(t)} - \lfloor \eta \rfloor \tilde{x}_i^{(t)}$. If η is an integer, then

$E(\tilde{x}'_i^{(t)}) = 0$; otherwise, $E(\tilde{x}'_i^{(t)}) = \lceil \eta \rceil \tilde{x}_i^{(t)} - \lfloor \eta \rfloor \tilde{x}_i^{(t)} = \tilde{x}_i^{(t)}$. In Line 8 through 18, we select a pair of fractions and round them in either Line 11-12 or Line 13-14. To guarantee no constraint violation, note that we have, for example, $\tilde{x}''_{i_1}^{(t)} |D_{i_1}^{(t)}| + \tilde{x}''_{i_2}^{(t)} |D_{i_2}^{(t)}| = (\tilde{x}'_{i_1}^{(t)} + \rho_1) |D_{i_1}^{(t)}| + (\tilde{x}'_{i_2}^{(t)} - k\rho_1) |D_{i_2}^{(t)}| = \tilde{x}'_{i_1}^{(t)} |D_{i_1}^{(t)}| + \tilde{x}'_{i_2}^{(t)} |D_{i_2}^{(t)}|$. To preserve the expectation, we have, for every i , that $E(\tilde{x}''_i^{(t)}) = (\eta - \lfloor \eta \rfloor) \frac{\rho_2}{\rho_1 + \rho_2} (\omega_1 \tilde{x}_i^{(t)} + \rho_1) + (\eta - \lfloor \eta \rfloor) \frac{\rho_1}{\rho_1 + \rho_2} (\omega_1 \tilde{x}_i^{(t)} - \rho_2) + (\lceil \eta \rceil - \eta) \frac{\rho_2}{\rho_1 + \rho_2} (\omega_2 \tilde{x}_i^{(t)} + \rho_1) + (\lceil \eta \rceil - \eta) \frac{\rho_1}{\rho_1 + \rho_2} (\omega_2 \tilde{x}_i^{(t)} - \rho_2) = \tilde{x}_i^{(t)}$, and it is the same for the other case (i.e., $\tilde{x}''_i^{(t)}$ changes to $\tilde{x}''_i^{(t)} - k\rho_1$ and $\tilde{x}''_i^{(t)} + k\rho_2$). ρ'_1 and ρ'_2 are computed similarly as ρ_1 and ρ_2 . Algorithm 3 has the time complexity of $O(I)$. We need I iterations for the loop at most, because at least one fraction is rounded in each iteration and there are I fractions to be rounded at most.

C. Regret and Fit Analysis

Dynamic Regret and Dynamic Fit: We introduce “dynamic regret” and “dynamic fit” [22], [25] as the performance metrics for our algorithms.

The dynamic regret measures the cumulative difference between the objective evaluated with the online solutions and the offline optimum. The dynamic regrets with regards to our original problem and its relaxed problem are as follows:

$$\begin{aligned} \text{Dreg}^{(T)} &:= E[\sum_{t=1}^T f^{(t)}(\bar{\mathbf{X}}^{(t)})] - \sum_{t=1}^T f^{(t)}(\mathbf{X}^{(t)*}), \\ \widetilde{\text{Dreg}}^{(T)} &:= \sum_{t=1}^T f^{(t)}(\tilde{\mathbf{X}}^{(t)}) - \sum_{t=1}^T f^{(t)}(\tilde{\mathbf{X}}^{(t)*}), \end{aligned}$$

where $\mathbf{X}^{(t)*}$ is the mixed-integer optimal solution, $\mathbf{X}^{(t)*} \in \arg \min_{\mathbf{X}^{(t)} \in \mathcal{X}^{(t)}} f^{(t)}(\mathbf{X}^{(t)})$, and $\tilde{\mathbf{X}}^{(t)*}$ is the fractional optimal solution, $\tilde{\mathbf{X}}^{(t)*} \in \arg \min_{\mathbf{X}^{(t)} \in \tilde{\mathcal{X}}^{(t)}} f^{(t)}(\mathbf{X}^{(t)})$. Their corresponding domains are $\mathcal{X}^{(t)} := \{\mathbf{X} \mid g^{(t)}(\mathbf{X}) \preceq \mathbf{0}, h^{(t)}(\mathbf{X}) \geq 0; x_i^{(t)} \in \{0, 1\}, \forall i; K_g(\delta^{(t)}) > 1\}$; $\tilde{\mathcal{X}}^{(t)} := \{\mathbf{X} \mid g^{(t)}(\mathbf{X}) \preceq \mathbf{0}, h^{(t)}(\mathbf{X}) \geq 0; x_i^{(t)} \in [0, 1], \forall i; K_g(\delta^{(t)}) > 1\}$.

The dynamic fit measures the cumulative violation of the long-term constraints evaluated with the online solutions. The dynamic fit with regards to our original problem and its relaxed problem are as follows, where $[\cdot]^+ = \max\{\cdot, 0\}$:

$$\begin{aligned} \text{Dfit}^{(T)} &:= \| [E[\sum_{t=1}^T g^{(t)}(\bar{\mathbf{X}}^{(t)})]]^+ \|, \\ \widetilde{\text{Dfit}}^{(T)} &:= \| [\sum_{t=1}^T g^{(t)}(\tilde{\mathbf{X}}^{(t)})]^+ \|. \end{aligned}$$

Regret and Fit Analysis: Our analysis is to rigorously show that both the dynamic regret and the dynamic fit evaluated with the online solutions from Algorithm 3 (which takes the output of Algorithm 2 as input) with regards to our original problem grow only sublinearly along with the length of the entire time horizon T . Towards that end, we make some assumptions that are also often made for a wide range of similar problems in general [6], [21], [22], [25]: (1) the functions $f^{(t)}(\tilde{\mathbf{X}})$ have bounded gradients on $\tilde{\mathcal{X}}$, i.e., $\|\nabla f^{(t)}(\tilde{\mathbf{X}})\| \leq G$, and $g^{(t)}(\tilde{\mathbf{X}})$ is also bounded on $\tilde{\mathcal{X}}$, i.e., $\|g^{(t)}(\tilde{\mathbf{X}})\| \leq D, \forall t$; (2) the radius of the convex feasible set $\tilde{\mathcal{X}}$ is bounded, i.e., $\|\tilde{\mathbf{X}}_1 - \tilde{\mathbf{X}}_2\| \leq R, \forall \tilde{\mathbf{X}}_1, \tilde{\mathbf{X}}_2 \in \tilde{\mathcal{X}}$; (3) there exists a constant $\varepsilon > 0$ and an interior point $\tilde{\mathbf{X}} \in \tilde{\mathcal{X}}$, such that $g^{(t)}(\tilde{\mathbf{X}}) \preceq -\varepsilon \mathbf{1}, \forall t$; (4) the

slack constant ε is larger than the point-wise maximal variation of the consecutive constraints, i.e., $\varepsilon > \bar{\mathcal{V}}(g)$, where $\bar{\mathcal{V}}(g) = \max_t \mathcal{V}_{g^{(t)}}$ and $\mathcal{V}_{g^{(t)}} = \max_{\tilde{\mathbf{X}} \in \tilde{\mathcal{X}}} \| [g^{(t+1)}(\tilde{\mathbf{X}}) - g^{(t)}(\tilde{\mathbf{X}})]^+ \|$. Based on all these assumptions, we derive the following results to quantify the dynamic regret and the dynamic fit:

Theorem 1. *We have $\text{Dreg}^{(T)} \leq \widetilde{\text{Dreg}}^{(T)}$ and $\text{Dfit}^{(T)} \leq \widetilde{\text{Dfit}}^{(T)} + \mathcal{N}\sigma_\beta^\beta$, where \mathcal{N} and σ_β^β are constants from Jensen Gap [37].*

Proof. See Appendix A. \square

Theorem 2. *The dynamic regret can be yielded as $\text{Dreg}^{(T)} \leq \widetilde{\text{Dreg}}^{(T)} \leq \frac{R^2 + R\mathcal{V}_{\tilde{\mathbf{X}}^{(t)*}}^T}{\alpha} + \frac{T\mu D^2}{2} + 2\alpha G^2 T + 2\alpha[(D^2 - (\frac{\Omega_{\max}}{\varepsilon})^2)^4] \mathcal{V}_{\lambda^{(t)}}^T$, where $\mathcal{V}_{\lambda^{(t)}}^T = \sum_t^T \|\lambda^{(t)}\|^2$ and $\mathcal{V}_{\tilde{\mathbf{X}}^{(t)*}}^T = \sum_{t=2}^T \|\tilde{\mathbf{X}}^{(t-1)*} - \tilde{\mathbf{X}}^{(t)*}\|$. The dynamic fit can be yielded as $\text{Dfit}^{(T)} \leq \widetilde{\text{Dfit}}^{(T)} + \mathcal{N}\sigma_\beta^\beta \leq \frac{\|\bar{\lambda}\|}{\mu} + \mathcal{N}\sigma_\beta^\beta$, where $\|\bar{\lambda}\| = \mu D + \frac{2GR + R^2/(2\alpha) + (\mu D^2)/2}{\varepsilon - \bar{\mathcal{V}}(g)}$.*

Proof. See Appendix B. \square

Corollary 1. *The dynamic regret and the dynamic fit can be written as follows, for $\alpha = \mu = \max\{\sqrt{\frac{\mathcal{V}_{\tilde{\mathbf{X}}^{(t)*}}^T}{T}}, \sqrt{\frac{\mathcal{V}_{\lambda^{(t)}}^T}{T}}\}$: $\text{Dreg}^{(T)} \leq \mathcal{O}(\max\{\sqrt{\mathcal{V}_{\tilde{\mathbf{X}}^{(t)*}}^T T}, \sqrt{\mathcal{V}_{\lambda^{(t)}}^T T}\}), \text{Dfit}^{(T)} \leq \mathcal{O}(\max\{\frac{T}{\mathcal{V}_{\tilde{\mathbf{X}}^{(t)*}}^T}, \frac{T}{\mathcal{V}_{\lambda^{(t)}}^T}\}) + \mathcal{N}\sigma_\beta^\beta$. If we further set $\alpha = \mu = \mathcal{O}(T^{-\frac{1}{3}})$, they can be expressed respectively as: $\text{Dreg}^{(T)} \leq \mathcal{O}(\max\{\mathcal{V}_{\tilde{\mathbf{X}}^{(t)*}}^T T^{\frac{1}{3}}, \mathcal{V}_{\lambda^{(t)}}^T T^{-\frac{1}{3}}, T^{\frac{2}{3}}\}), \text{Dfit}^{(T)} \leq \mathcal{O}(T^{\frac{2}{3}}) + \mathcal{N}\sigma_\beta^\beta$.*

V. ONLINE PAYMENT ALLOCATION

We design the payment allocation algorithm for calculating the remuneration for the selected bidders. We also define truthfulness and individual rationality, and prove that our proposed approach satisfies these two economic properties.

A. Payment Allocation Algorithm

Algorithm 4 presents the payment calculation in our online auction mechanism. The auctions are randomized, because we determine the winning bids in each auction by Algorithm 3 in a randomized manner. Using $\tilde{x}_i^{(t)}(c_i^{(t)}, \mathbf{c}_{-i}^{(t)})$ to denote the fractional solutions output by Algorithm 2 where the bid i reports its cost as $c_i^{(t)}$ and the other bids report $\mathbf{c}_{-i}^{(t)}$, we take an integral up to the upper bound of $\kappa_i^{(t)} = \mathcal{V} \log_2(\frac{1}{\theta_i^{(t)}}) M \zeta_1^{(t)} + |D_i^{(t)}| \zeta_2^{(t)}$, where $\zeta_1^{(t)}$ has been explained before and $\zeta_2^{(t)}$ can be the estimated unit valuation of the training data as if such data were offered by the server itself. This upper bound captures the maximum unit payment the server can tolerate and can make to the corresponding bid. Algorithm 4 has the time complexity of $O(I \cdot n \cdot I^2 \log(1/\epsilon))$. For the first loop, we have I iterations. In each iteration, to calculate the numerical integration, we suppose we divide the range of $\kappa_i^{(t)} - c_i^{(t)}$ into n segments and for each segment we need to use Algorithm 2 to obtain the fractional bid-selection decision $\tilde{x}_i^{(t)}(c, \mathbf{c}_{-i}^{(t)})$.

Algorithm 4: Payment Allocation Algorithm

Input: Winner set $[\bar{x}_1^{(t)}, \dots, \bar{x}_I^{(t)}]$
Output: payment $r_i^{(t)}, \forall i$

- 1 **for** i , where $\bar{x}_i^{(t)} = 1$ **do**
 - 2 Set $r_i^{(t)} = c_i^{(t)} \tilde{x}_i^{(t)}(c_i^{(t)}, \mathbf{c}_{-i}^{(t)}) + \int_{c_i^{(t)}}^{\kappa_i^{(t)}} \tilde{x}_i^{(t)}(c, \mathbf{c}_{-i}^{(t)}) dc$;
 - 3 **for** i , where $\bar{x}_i^{(t)} = 0$ **do**
 - 4 Set $r_i^{(t)} = 0$;

B. Economic Properties Analysis

We define “utility”, and based on it, we define “truthfulness” and “individual rationality” as the two economic properties.

Definition 1. Utility. *The utility of the bid i at the time slot t is*

$$u_i(b_i^{(t)}, \mathbf{b}_{-i}^{(t)}) = \begin{cases} r_i^{(t)}(b_i^{(t)}, \mathbf{b}_{-i}^{(t)}) - c_i^{(t)} E(\bar{x}_i^{(t)}(b_i^{(t)}, \mathbf{b}_{-i}^{(t)})), & \text{if } \bar{x}_i^{(t)} = 1 \\ 0, & \text{otherwise} \end{cases}$$

where $b_i^{(t)}$ is the bidding price, $\mathbf{b}_{-i}^{(t)}$ refers to the bidding prices of all the other bids except the bid i .

Definition 2. Truthfulness. *A randomized auction is truthful in expectation if every bid i maximizes its expected utility by bidding its truth cost $c_i^{(t)}$, i.e., $u_i(c_i^{(t)}, \mathbf{b}_{-i}^{(t)}) \geq u_i(b_i^{(t)}, \mathbf{b}_{-i}^{(t)})$.*

Definition 3. Individual Rationality. *A randomized auction is individually rational in expectation if every bid i always has a non-negative utility, i.e., $u_i(b_i^{(t)}, \mathbf{b}_{-i}^{(t)}) \geq 0$.*

Truthfulness and Individual Rationality Analysis: We present the following theorem, which firstly states the sufficient and necessary conditions [38] for a randomized auction to become truthful and individually rational and then highlights that our proposed auction meets such conditions indeed.

Theorem 3. *A randomized auction is truthful and individually rational in expectation by satisfying the following conditions: (1) $E(\bar{x}_i^{(t)})$ is monotonically non-increasing in $c_i^{(t)}, \forall i$; (2) $\int_0^\infty E(\bar{x}_i^{(t)}) dc < \infty, \forall i$; (3) the payment is in the form as follows: $r_i^{(t)} = c_i^{(t)} E(\bar{x}_i^{(t)}(c_i^{(t)}, \mathbf{c}_{-i}^{(t)})) + \int_{c_i^{(t)}}^\infty E(\bar{x}_i^{(t)}(c, \mathbf{c}_{-i}^{(t)})) dc, \forall i$. Our proposed auction meets these conditions.*

Proof. See Appendix C. \square

Note that the key to satisfy the conditions in Theorem 3 is to ensure $E(\bar{x}_i^{(t)}) = \tilde{x}_i^{(t)}, \forall i$, where $\tilde{x}_i^{(t)}, \forall i$ is the fractional solution optimally solved from the one-slice problem at t . We achieve this jointly through our Online Fractional Algorithm and our Randomized Rounding Algorithm.

VI. EXPERIMENTAL STUDY

In this section, we conduct multiple trace-driven experiments to evaluate the performance of our proposed FLORA and interpret all the experimental results.

A. Experimental Settings

Training Data and Tasks: We utilize the handwritten digit classification dataset, MNIST [39], and the image classification dataset, Fashion-MNIST [40] for federated learning. Both datasets contain 28×28 gray-scale images in 10 classes, a training set of 60,000 examples and a test set of 10,000 examples. We summarize the specific training tasks in our experiments as follows.

MNIST_MLP: This task trains Multi-Layer Perception (MLP) model on MNIST. The MLP is composed as follows: a fully connected layer as the input layer; followed by ReLU activation; a drop-out layer with $d = 0.5$ (i.e., dropout rate); another fully connected layer as the hidden layer; and a final softmax output layer.

MNIST_CNN: This task trains Convolutional Neural Network (CNN) model on MNIST. The CNN consists of the following structure: two 3×3 convolution layers (the first layer with 16 channels and the second layer with 32 channels), each followed by ReLU activation and 2×2 max pooling; a fully connected layer; and a final softmax output layer.

FMNIST_MLR: This task trains Multinomial Logistic Regression (MLR) model on Fashion-MNIST. The MLR model consists of a fully connected layer and a softmax output layer.

Server, Devices, and Bids: We set one federated learning server, and vary the number of mobile devices as $|\mathcal{I}| = 10 \sim 80$. We consider a time horizon of $|\mathcal{T}| = 6000$ minutes, with 60 minutes as one time slot. We set most of the inputs as values randomly taken from realistic ranges: the asking price $c_i^{(t)}$ for each round of local iteration is from $[5, 15]$ \$; the energy per unit communication γ_i is from $[0.04, 0.08]$ mWh; the cost per unit computation $\zeta_1^{(t)}$ is from $[0.02, 0.04]$ \$; the battery capacity Ω_i is from $[20, 150]$ Wh; the valuation per unit data at the server $\zeta_2^{(t)}$ is from $[0.2, 0.3]$ \$/Mbits; the local accuracy $\theta_i^{(t)}$ is from $[0.2, 0.9]$ [1]; the transmission power $p_i^{(t)}$ is from $[2, 20]$ dBm; and the channel gain $hp_i^{(t)}$ is from $[-90, -95]$ dB [1]. We assume that the noise power spectral density is $N_0 = -174$ dBm/Hz [6] and that the bandwidth B is 25 kHz.

Federated Learning: We emulate the federated learning by executing different image classification tasks, where we execute a single task in each single time slot.

- **Implementation:** We implement the federated learning algorithm shown in Section III, and construct the federated learning framework using PyTorch [41] (Version 1.7.0) as the training pipeline. We conduct our experiments on a desktop server with an Intel Xeon E5 CPU, 32GB RAM, 2TB HDD, 512GB SSD, and the Linux Ubuntu 16.04 operating system.
- **Data Distribution:** To capture the heterogeneous nature of the federated learning environment, we note that the training data a client has may not be representative for the data's population distribution and that the amount of data each client has may also be different. Thus, we partition the entire dataset and assign the partitions to the clients as in the “non-IID and unbalanced” setting and the “IID and balanced” setting [42], respectively, where “IID” refers to “Independent and Identically Distributed”. For the unbalanced distribution, we assign different amounts

of data according to the power law [43]. For the non-IID distribution, we assign each client the samples with 3 labels for the MNIST dataset and 4 labels for the Fashion-MNIST dataset. Due to the power law we use, the range of the amount of the data samples used in our experiments is from [30, 4380] for MNIST and [37, 1133] for Fashion-MNIST [43]. We train each model on the entire 10,000 test samples.

- **Hyperparameters:** We use the Negative Log Likelihood Loss (NLLLoss) function as our loss function. We set the batch size of data as 20 and the hyper-learning rate [33] as 0.07. For the learning tasks MNIST_MLP, MNIST_CNN, and FMNIST_MLR, we set the corresponding learning rates as 0.003, 0.0002, and 0.001, respectively.

Control Algorithms: We implement and compare multiple approaches that select bids and control federated learning over time: (1) **FLORA**, our online approach proposed in this paper; (2) **Random_FL**, the algorithm that selects bids randomly at each time slot until the total amount of training data reaches the required threshold; (3) **Greedy_FL**, the algorithm that always select the bids with the lowest energy consumption per global iteration, regardless of the social cost, at each time slot; (4) **Fixed_FL** [44], the algorithm that selects the bid i whose asking price is no more than $p_f \cdot |D_i^{(t)}|$, where p_f is the fixed price for one unit of data size; (5) **NoA_FL**, the algorithm that uses all the available bids at each time slot without selection; (6) **Offline**, the approach that knows all the inputs over the entire time horizon in advance and solves social cost minimization for the fractional solutions via the optimization solver CasADi [45]. Here, note that solving our nonlinear mixed-integer program with state-of-the-art solvers still takes unacceptably long time; thus, we use the offline optimal fractional solutions as a lower bound for the offline optimal mixed-integer solutions to our problem.

B. Experimental Results

Social Cost: Fig. 2 visualizes the normalized cumulative social cost of different algorithms across continuous time slots when the number of bids and the target accuracy are fixed. We observe that our FLORA algorithm shows a slower growth trend in terms of the cumulative social cost than Random_FL, Greedy_FL and Fixed_FL, and is closer to the performance of the Offline algorithm.

Scalability: Fig. 3 depicts the normalized cumulative social cost of different algorithms as the function of the number of the bidders. FLORA beats Random_FL, Fixed_FL and Greedy_FL, saving up to 38.9%, 29.0% and 42.1% social cost on average, respectively. We see that the more participants there are, the more opportunities the server has with FLORA in choosing the winning bids with high quality and low price to reduce the social cost of the entire system, which validates the scalability of our approach.

Individual Rationality and Truthfulness: Fig. 4 and Fig. 5 exhibit two randomly-chosen bids with their received payments. In Fig. 4, through auctions in different time slots, the received payment is always no less than the bidding price (and the payment is zero by default when a bid loses in an auction).

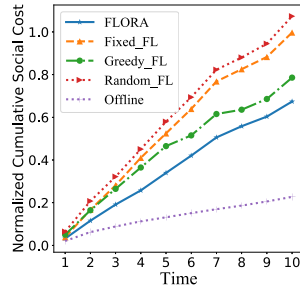


Fig. 2: Social cost

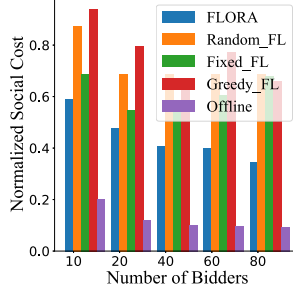


Fig. 3: Scalability

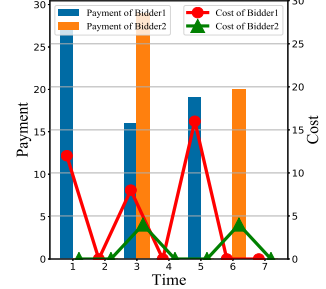


Fig. 4: Payment vs. cost

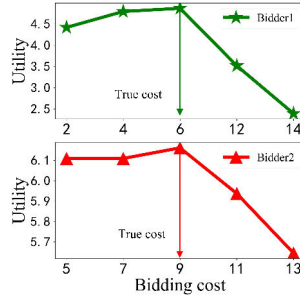


Fig. 5: Utility

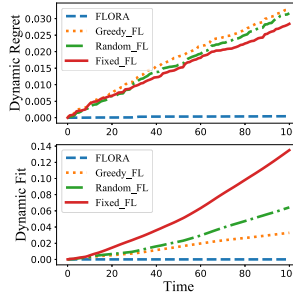


Fig. 6: Dynamic regret & fit

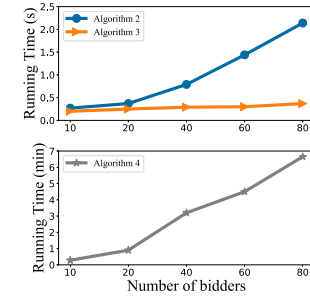


Fig. 7: Algorithm running time

Thus, individual rationality is achieved. In Fig. 5, we see that if a bid bids the price other than its true cost (given all the other bids unchanged), it cannot achieve the maximum utility. Thus, truthfulness is achieved.

Dynamic Regret and Dynamic Fit: Fig. 6 shows the dynamic regret and the dynamic fit for all the algorithms, as the length of the entire time horizon changes. FLORA presents the lowest dynamic regret and fit. This figure also confirms that both the regret and the fit of FLORA grow sublinearly in practice along with time, aligning with our theoretical analysis.

Algorithm running time: Fig. 7 depicts the execution time of our Online Fractional Algorithm (i.e., Algorithm 2), Randomized Rounding Algorithm (i.e., Algorithm 3), and Payment Allocation Algorithm (i.e., Algorithm 4). Even as the number of bidders reaches 80, Algorithm 2, 3, and 4 can finish within 2.2s, 0.5s, and 7min for each auction, respectively. Our proposed algorithms are computationally efficient in practice. We consider such execution time negligible in realistic scenarios, compared to the time duration of a single time slot.

Empirical Quality of Models: Fig. 8 presents the inference accuracy and the loss of the models trained by FLORA and output at each time slot in the non-IID and unbalanced setting and the IID and balanced setting, respectively, validating the robustness and applicability of FLORA in the heterogeneous federated learning environment. The results are obtained for the same global iterations ($K_g = 500$), local iterations ($K_l = 10$), and clients ($|\mathcal{I}| = 100$) for the training tasks of MNIST_MLP, MNIST_CNN, and FMNIST_MLR. The results show a good convergence trend, even in the non-IID and unbalanced setting, and indicate that FLORA can always control federated learning to achieve satisfiable inference accuracy and loss. Here, note that, we are not doing any fine tune of the (hyper)parameters of MLP, CNN, and MLR models; the inference accuracy and loss can be made even

better if one continues to tune such (hyper)parameters. In the non-IID and unbalanced setting, the average inference accuracy of MNIST_MLP, MNIST_CNN, and FMNIST_MLR is 85.78%, 83.72% and 78.35%, respectively; in the IID and balanced setting, the average inference accuracy of MNIST_MLP, MNIST_CNN, and FMNIST_MLR is 90.13%, 84.02% and 80.45%, respectively, which validating that FLORA ensures low loss and high accuracy across different training tasks with the different data distribution.

Social Cost and Training Time: We present our experimental results on the social cost for different training tasks and the total training time consumed by federated learning over an entire process of model training for the five algorithms, FLORA, Random_FL, Greedy_FL, Fixed_FL and NoA_FL, respectively. We set $|\mathcal{I}| = 100$ clients with the target global accuracies of 0.82, 0.80, and 0.78 for MNIST_MLP, MNIST_CNN, and FMNIST_MLR, respectively. Fig. 9 demonstrates that our algorithm can always guarantee the lowest social cost. Fig. 10 presents the comparison of total training time, decided by the local iterations and the global iterations. For reaching the same target global accuracy, the shorter the training time is, the higher the training efficiency is.

VII. CONCLUSION

In this paper, we conduct an algorithmic study of incentivizing mobile devices to participate in federated learning, subject to their long-term energy constraints. We design a mechanism of repetitive auctions, jointly using three algorithms to select the winning bids and allocating the corresponding payments in an online and randomized manner without requiring the knowledge of any future inputs. We formally prove the sublinear regret and fit for our approach regarding its long-term performance, and prove the economic properties of truthfulness and individual rationality regarding each single auction. We

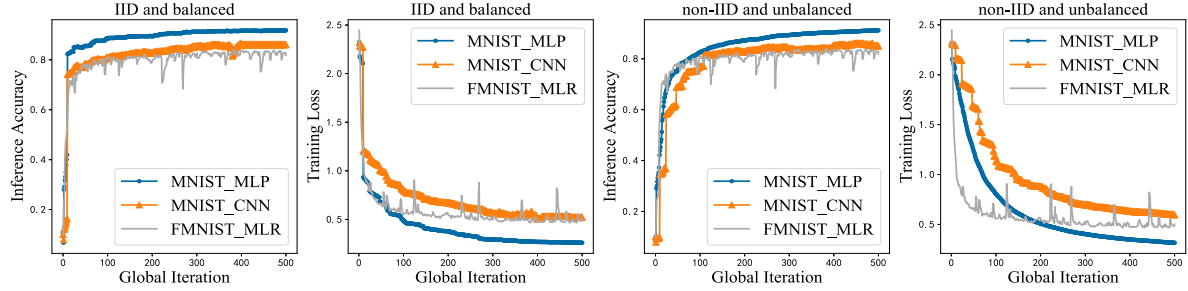


Fig. 8: Accuracy and loss in the IID and balanced setting and the non-IID and unbalanced setting

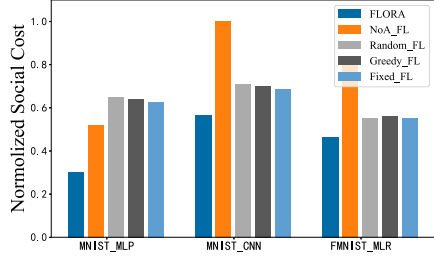


Fig. 9: Social cost

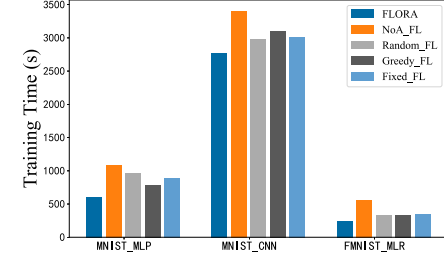


Fig. 10: Training time

have also carried out extensive experiments and demonstrated the results in many different aspects to validate the practical performance of our proposed approach.

APPENDIX

A. Proof of Theorem 1

We derive the relationship between $\text{Dreg}^{(T)}$ and $\widetilde{\text{Dreg}}^{(T)}$ as

$$\begin{aligned} E\left[\sum_{t=1}^T f(\mathbf{X}^{(t)})\right] - \sum_{t=1}^T f(\mathbf{X}^{(t)*}) &\stackrel{8(a)}{=} \sum_{t=1}^T f(E[\mathbf{X}^{(t)}]) - \sum_{t=1}^T f(\mathbf{X}^{(t)*}) \\ &= \sum_{t=1}^T f(\tilde{\mathbf{X}}^{(t)}) - \sum_{t=1}^T f(\mathbf{X}^{(t)*}) + \sum_{t=1}^T f(E[\mathbf{X}^{(t)}]) - \sum_{t=1}^T f(\tilde{\mathbf{X}}^{(t)}) \\ &\stackrel{8(b)}{\leq} \sum_{t=1}^T f(\tilde{\mathbf{X}}^{(t)}) - \sum_{t=1}^T f(\tilde{\mathbf{X}}^{(t)*}) = \widetilde{\text{Dreg}}^{(T)}, \end{aligned} \quad (8)$$

where 8(a) holds by the linearity of $f(\mathbf{X}^{(t)})$, 8(b) holds due to $E[\mathbf{X}^{(t)}] = \tilde{\mathbf{X}}^{(t)}$ which ensured by randomized rounding algorithm and the fact that the objective value conducted by integer optimum is more than fractional optimum. We derive dynamic fit $\text{Dfit}^{(T)}$ as

$$\begin{aligned} \text{Dfit}^{(T)} &= \left\| [E\left[\sum_{t=1}^T g^{(t)}(\mathbf{X}^{(t)})\right]]^+ \right\| \stackrel{9(a)}{\leq} \left\| E\left[\sum_{t=1}^T g^{(t)}(\mathbf{X}^{(t)})\right]\right\| \\ &\stackrel{9(b)}{\leq} \left\| \sum_{t=1}^T g^{(t)}(E[\mathbf{X}^{(t)}]) + \mathcal{N}\sigma_\beta^\beta \right\| = \left\| \sum_{t=1}^T g^{(t)}(\tilde{\mathbf{X}}^{(t)}) + \mathcal{N}\sigma_\beta^\beta \right\| \\ &\leq \left\| \sum_{t=1}^T g^{(t)}(\tilde{\mathbf{X}}^{(t)}) \right\| + \left\| \mathcal{N}\sigma_\beta^\beta \right\| = \widetilde{\text{Dfit}}^{(T)} + \mathcal{N}\sigma_\beta^\beta, \end{aligned} \quad (9)$$

where 9(a) follows that the value of 2-Norm will decrease due to all the negative values are set to 0 by using $[\cdot]^+ = \max\{\cdot, 0\}$. Jensen Gap, the linearity of $g^{(t)}(\mathbf{X}^{(t)})$ and the unchanged expectation property holds by the randomized rounding algorithm guarantee 9(b), where \mathcal{N} and σ_β^β are the constants introduced by Jensen Gap [6], [37].

Lemma 1. Under the all assumption, for and $\tilde{\mathbf{X}}^{(t)} \in \tilde{\mathcal{X}}^{(t)}$, we have

$$\begin{aligned} &\nabla_{\mathbf{X}} \mathcal{L}^{(t)}(\tilde{\mathbf{X}}^{(t)}, \lambda^{(t)})(\tilde{\mathbf{X}}^{(t)} - \tilde{\mathbf{X}}^{(t)*}) \\ &\leq \frac{[\|\tilde{\mathbf{X}}^{(t)*} - \tilde{\mathbf{X}}^{(t)}\|^2 - \|\tilde{\mathbf{X}}^{(t)*} - \tilde{\mathbf{X}}^{(t+1)}\|^2]}{2\alpha} + \frac{\alpha[\|\nabla_{\mathbf{X}} \mathcal{L}^{(t)}(\tilde{\mathbf{X}}^{(t)}, \lambda^{(t)})\|^2]}{2}. \end{aligned} \quad (10)$$

The corresponding bound for the dual variables holds:

$$\begin{aligned} &\nabla_{\lambda} \mathcal{L}^{(t)}(\tilde{\mathbf{X}}^{(t)}, \lambda^{(t)})(\tilde{\mathbf{X}}^{(t)} - \tilde{\mathbf{X}}^{(t)*}) \\ &\leq \frac{[\|\lambda - \lambda^{(t)}\|^2 - \|\lambda - \lambda^{(t+1)}\|^2]}{2\mu} + \frac{\mu[\|\nabla_{\lambda} \mathcal{L}^{(t)}(\tilde{\mathbf{X}}^{(t)}, \lambda^{(t)})\|^2]}{2}. \end{aligned} \quad (11)$$

Proof. Given the primal input $\tilde{\mathbf{X}}^{(t)*}$ and dual iterate $\lambda^{(t)}$, the optimal decision $\tilde{\mathbf{X}}^{(t+1)}$ at $t+1$ is obtained by

$$\begin{aligned} &\min_{\tilde{\mathbf{X}}^{(t)} \in \tilde{\mathcal{X}}^{(t)}} \nabla_{\mathbf{X}} \mathcal{L}^{(t)}(\tilde{\mathbf{X}}^{(t)}, \lambda^{(t)})(\tilde{\mathbf{X}}^{(t)} - \tilde{\mathbf{X}}^{(t)*}) + \frac{1}{2\alpha} \|\tilde{\mathbf{X}}^{(t)} - \tilde{\mathbf{X}}^{(t)*}\|^2, \\ &\text{s.t.} \\ &\quad h^{(t)}(\tilde{\mathbf{X}}^{(t)}) \geq 0 \end{aligned}$$

So, the optimal condition implies [25]

$$(\tilde{\mathbf{X}}^{(t)*} - \tilde{\mathbf{X}}^{(t+1)}) \cdot (\alpha \nabla_{\mathbf{X}} \mathcal{L}^{(t)}(\tilde{\mathbf{X}}^{(t)}, \lambda^{(t)}) + \tilde{\mathbf{X}}^{(t+1)} - \tilde{\mathbf{X}}^{(t)}) \geq 0. \quad (12)$$

Firstly, we focus on the item $\alpha(\tilde{\mathbf{X}}^{(t)} - \tilde{\mathbf{X}}^{(t)*}) \nabla_{\mathbf{X}} \mathcal{L}^{(t)}(\tilde{\mathbf{X}}^{(t)}, \lambda^{(t)})$:

$$\begin{aligned} &\alpha(\tilde{\mathbf{X}}^{(t)} - \tilde{\mathbf{X}}^{(t)*}) \nabla_{\mathbf{X}} \mathcal{L}^{(t)}(\tilde{\mathbf{X}}^{(t)}, \lambda^{(t)}) \\ &= \alpha(\tilde{\mathbf{X}}^{(t+1)} - \tilde{\mathbf{X}}^{(t)*}) \nabla_{\mathbf{X}} \mathcal{L}^{(t)}(\tilde{\mathbf{X}}^{(t)}, \lambda^{(t)}) + \\ &\quad \alpha(\tilde{\mathbf{X}}^{(t)} - \tilde{\mathbf{X}}^{(t+1)}) \nabla_{\mathbf{X}} \mathcal{L}^{(t)}(\tilde{\mathbf{X}}^{(t)}, \lambda^{(t)}) \\ &\stackrel{13(a)}{\leq} \alpha(\tilde{\mathbf{X}}^{(t)} - \tilde{\mathbf{X}}^{(t+1)}) \nabla_{\mathbf{X}} \mathcal{L}^{(t)}(\tilde{\mathbf{X}}^{(t)}, \lambda^{(t)}) + \\ &\quad (\tilde{\mathbf{X}}^{(t)*} - \tilde{\mathbf{X}}^{(t+1)}) (\tilde{\mathbf{X}}^{(t+1)} - \tilde{\mathbf{X}}^{(t)}), \end{aligned} \quad (13)$$

where 13(a) holds by the inequality (12). For $\alpha(\tilde{\mathbf{X}}^{(t)} - \tilde{\mathbf{X}}^{(t+1)}) \nabla_{\mathbf{X}} \mathcal{L}^{(t)}(\tilde{\mathbf{X}}^{(t)}, \lambda^{(t)})$, we have

$$\begin{aligned} &\alpha(\tilde{\mathbf{X}}^{(t)} - \tilde{\mathbf{X}}^{(t+1)}) \nabla_{\mathbf{X}} \mathcal{L}^{(t)}(\tilde{\mathbf{X}}^{(t)}, \lambda^{(t)}) \\ &\stackrel{14(a)}{\leq} \alpha \|\tilde{\mathbf{X}}^{(t)} - \tilde{\mathbf{X}}^{(t+1)}\| \|\nabla_{\mathbf{X}} \mathcal{L}^{(t)}(\tilde{\mathbf{X}}^{(t)}, \lambda^{(t)})\| \\ &\stackrel{14(b)}{\leq} \frac{1}{2} \|\tilde{\mathbf{X}}^{(t)} - \tilde{\mathbf{X}}^{(t+1)}\|^2 + \frac{\alpha^2}{2} \|\nabla_{\mathbf{X}} \mathcal{L}^{(t)}(\tilde{\mathbf{X}}^{(t)}, \lambda^{(t)})\|^2. \end{aligned} \quad (14)$$

According to Cauchy-Schwartz inequality, we obtain 14(a). 14(b) holds by Young's inequality. Then we focus on $(\tilde{\mathbf{X}}^{(t)*} - \tilde{\mathbf{X}}^{(t+1)})(\tilde{\mathbf{X}}^{(t+1)} - \tilde{\mathbf{X}}^{(t)})$, we have

$$\begin{aligned} & (\tilde{\mathbf{X}}^{(t)*} - \tilde{\mathbf{X}}^{(t+1)})(\tilde{\mathbf{X}}^{(t+1)} - \tilde{\mathbf{X}}^{(t)}) \\ & \leq \frac{1}{2} \|\tilde{\mathbf{X}}^{(t)*} - \tilde{\mathbf{X}}^{(t)}\|^2 - \frac{1}{2} \|\tilde{\mathbf{X}}^{(t+1)} - \tilde{\mathbf{X}}^{(t)}\|^2 - \frac{1}{2} \|\tilde{\mathbf{X}}^{(t)*} - \tilde{\mathbf{X}}^{(t+1)}\|^2. \end{aligned} \quad (15)$$

Based on the above, we can get (10) by plugging (14) and (15) into (13). Next, we continue the proof of (11): $\|\boldsymbol{\lambda} - \boldsymbol{\lambda}^{(t+1)}\|^2 = \|\boldsymbol{\lambda} - [\boldsymbol{\lambda}^{(t)} + \mu \nabla_{\boldsymbol{\lambda}} \mathcal{L}^{(t)}(\tilde{\mathbf{X}}^{(t)}, \boldsymbol{\lambda}^{(t)})]\|^2 \leq \|\boldsymbol{\lambda} - \boldsymbol{\lambda}^{(t)}\|^2 - 2\mu(\boldsymbol{\lambda} - \boldsymbol{\lambda}^{(t)})^\top \nabla_{\boldsymbol{\lambda}} \mathcal{L}^{(t)}(\tilde{\mathbf{X}}^{(t)}, \boldsymbol{\lambda}^{(t)}) + \mu^2 \|\nabla_{\boldsymbol{\lambda}} \mathcal{L}^{(t)}(\tilde{\mathbf{X}}^{(t)}, \boldsymbol{\lambda}^{(t)})\|^2$. Finally we rearrange the sequence, then obtain

$$\begin{aligned} & \nabla_{\boldsymbol{\lambda}} \mathcal{L}^{(t)}(\tilde{\mathbf{X}}^{(t)}, \boldsymbol{\lambda}^{(t)}) (\boldsymbol{\lambda} - \boldsymbol{\lambda}^{(t)}) \\ & \leq \frac{1}{2\mu} [\|\boldsymbol{\lambda} - \boldsymbol{\lambda}^{(t)}\|^2 - \|\boldsymbol{\lambda} - \boldsymbol{\lambda}^{(t+1)}\|^2] + \frac{\mu}{2} [\|\nabla_{\boldsymbol{\lambda}} \mathcal{L}^{(t)}(\tilde{\mathbf{X}}^{(t)}, \boldsymbol{\lambda}^{(t)})\|^2]. \end{aligned}$$

□

Lemma 2. Under the all assumptions and the update of primal and dual variables according to Algorithm 1, we have

$$\begin{aligned} & \mathcal{L}^{(t)}(\tilde{\mathbf{X}}^{(t)}, \boldsymbol{\lambda}) - \mathcal{L}^{(t)}(\tilde{\mathbf{X}}^{(t)*}, \boldsymbol{\lambda}^{(t)}) \\ & \leq \frac{\left[\|\tilde{\mathbf{X}}^{(t)*} - \tilde{\mathbf{X}}^{(t)}\|^2 - \|\tilde{\mathbf{X}}^{(t)*} - \tilde{\mathbf{X}}^{(t+1)}\|^2 \right]}{2\alpha} + \frac{\alpha \left[\|\nabla_{\boldsymbol{\lambda}} \mathcal{L}^{(t)}(\tilde{\mathbf{X}}^{(t)}, \boldsymbol{\lambda}^{(t)})\|^2 \right]}{2} \\ & \quad + \frac{\left[\|\boldsymbol{\lambda} - \boldsymbol{\lambda}^{(t)}\|^2 - \|\boldsymbol{\lambda} - \boldsymbol{\lambda}^{(t+1)}\|^2 \right]}{2\mu} + \frac{\mu \left[\|\nabla_{\boldsymbol{\lambda}} \mathcal{L}^{(t)}(\tilde{\mathbf{X}}^{(t)}, \boldsymbol{\lambda}^{(t)})\|^2 \right]}{2}. \end{aligned}$$

Proof. According to the convexity of $\mathcal{L}^{(t)}(\tilde{\mathbf{X}}^{(t)}, \boldsymbol{\lambda}^{(t)})$ w.r.t. $\boldsymbol{\lambda}^{(t)}$ and the concavity of $\mathcal{L}^{(t)}(\tilde{\mathbf{X}}^{(t)}, \boldsymbol{\lambda})$ w.r.t. $\boldsymbol{\lambda}$, we have $\mathcal{L}^{(t)}(\tilde{\mathbf{X}}^{(t)}, \boldsymbol{\lambda}^{(t)}) - \mathcal{L}^{(t)}(\tilde{\mathbf{X}}^{(t)*}, \boldsymbol{\lambda}^{(t)}) \leq \nabla_{\boldsymbol{\lambda}} \mathcal{L}^{(t)}(\tilde{\mathbf{X}}^{(t)}, \boldsymbol{\lambda}^{(t)})^\top (\tilde{\mathbf{X}}^{(t)} - \tilde{\mathbf{X}}^{(t)*})$, $\mathcal{L}^{(t)}(\tilde{\mathbf{X}}^{(t)}, \boldsymbol{\lambda}) - \mathcal{L}^{(t)}(\tilde{\mathbf{X}}^{(t)}, \boldsymbol{\lambda}^{(t)}) \leq (\boldsymbol{\lambda} - \boldsymbol{\lambda}^{(t)})^\top \nabla_{\boldsymbol{\lambda}} \mathcal{L}^{(t)}(\tilde{\mathbf{X}}^{(t)}, \boldsymbol{\lambda}^{(t)})$. Sum the above two inequalities, we obtain

$$\begin{aligned} & \mathcal{L}^{(t)}(\tilde{\mathbf{X}}^{(t)}, \boldsymbol{\lambda}) - \mathcal{L}^{(t)}(\tilde{\mathbf{X}}^{(t)*}, \boldsymbol{\lambda}^{(t)}) \\ & \leq \nabla_{\boldsymbol{\lambda}} \mathcal{L}^{(t)}(\tilde{\mathbf{X}}^{(t)}, \boldsymbol{\lambda}^{(t)})^\top (\tilde{\mathbf{X}}^{(t)} - \tilde{\mathbf{X}}^{(t)*}) + (\boldsymbol{\lambda} - \boldsymbol{\lambda}^{(t)})^\top \nabla_{\boldsymbol{\lambda}} \mathcal{L}^{(t)}(\tilde{\mathbf{X}}^{(t)}, \boldsymbol{\lambda}^{(t)}) \\ & \stackrel{16(a)}{\leq} \frac{1}{2\alpha} (\|\tilde{\mathbf{X}}^{(t)*} - \tilde{\mathbf{X}}^{(t)}\|^2 - \|\tilde{\mathbf{X}}^{(t)*} - \tilde{\mathbf{X}}^{(t+1)}\|^2) \\ & \quad + \frac{\alpha}{2} (\|\nabla_{\boldsymbol{\lambda}} \mathcal{L}^{(t)}(\tilde{\mathbf{X}}^{(t)}, \boldsymbol{\lambda}^{(t)})\|^2) \\ & \quad + \frac{1}{2\mu} (\|\boldsymbol{\lambda} - \boldsymbol{\lambda}^{(t)}\|^2 - \|\boldsymbol{\lambda} - \boldsymbol{\lambda}^{(t+1)}\|^2) + \frac{\mu}{2} (\|\nabla_{\boldsymbol{\lambda}} \mathcal{L}^{(t)}(\tilde{\mathbf{X}}^{(t)}, \boldsymbol{\lambda}^{(t)})\|^2), \end{aligned} \quad (16)$$

where 16(a) holds by Lemma 1. □

Lemma 3. We get the result over the entire time span under Lemma 1:

$$\begin{aligned} & \sum_t \mathcal{L}^{(t)}(\tilde{\mathbf{X}}^{(t)}, \boldsymbol{\lambda}) - \sum_t \mathcal{L}^{(t)}(\tilde{\mathbf{X}}^{(t)*}, \boldsymbol{\lambda}^{(t)}) \\ & \leq \frac{R^2 + R\mathcal{V}_{\tilde{\mathbf{X}}^{(t)*}}^T}{\alpha} + \frac{\|\boldsymbol{\lambda}\|^2}{2\mu} + \frac{T\mu D^2}{2} \\ & \quad + 2\alpha G^2 T + 2\alpha[(D^2 - (\frac{\Omega_{max}}{T})^2)^4] \mathcal{V}_{\boldsymbol{\lambda}^{(t)}}^T, \end{aligned}$$

where $\mathcal{V}_{\boldsymbol{\lambda}^{(t)}}^T = \sum_t \|\boldsymbol{\lambda}^{(t)}\|^2$.

Proof. Firstly, we focus on the term $\|g^{(t)}(\tilde{\mathbf{X}}^{(t)})\|$. According to the previous assumption (1):

$$\begin{aligned} & \|g^{(t)}(\tilde{\mathbf{X}}^{(t)})\| \leq D \Rightarrow \|Kg^{(t)} \cdot \mathbb{E}_i^{(t)} - \frac{\Omega_i}{T}\| \leq D, \forall i \\ & \Rightarrow D^2 \geq \|Kg^{(t)} \cdot \mathbb{E}_i^{(t)} - \frac{\Omega_i}{T}\|^2 = (Kg^{(t)} \cdot \mathbb{E}_i^{(t)})^2 + (\frac{\Omega_i}{T})^2, \forall i \\ & \Rightarrow D^2 \geq (Kg^{(t)} \cdot \mathbb{E}_{max}^{(t)})^2 + (\frac{\Omega_{max}}{T})^2 \\ & \Rightarrow (Kg^{(t)} \cdot \mathbb{E}_{max}^{(t)})^2 \\ & \leq D^2 - \frac{\Omega_{max}^2}{T^2}. \end{aligned} \quad (17)$$

Secondly, we focus on the term $\|\boldsymbol{\lambda}^{(t)} \nabla_{\boldsymbol{\lambda}} g^{(t)}(\tilde{\mathbf{X}}^{(t)})\|$. According to the constraints (3a) and (3b), we can get: $\boldsymbol{\lambda}^{(t)} \nabla_{\boldsymbol{\lambda}} g^{(t)}(\tilde{\mathbf{X}}^{(t)}) = [\boldsymbol{\lambda}_1^{(t)} K g^{(t)} \mathbb{E}_i^{(t)}, \dots, \boldsymbol{\lambda}_I^{(t)} K g^{(t)} \mathbb{E}_i^{(t)}, \boldsymbol{\lambda}_{I+1}^{(t)} K g^{(t)} \theta_{I+1}^{(t)}, \dots, \boldsymbol{\lambda}_{2I}^{(t)} K g^{(t)} \theta_{2I}^{(t)}]$

$$\begin{aligned} & \|\boldsymbol{\lambda}^{(t)} \nabla_{\boldsymbol{\lambda}} g^{(t)}(\tilde{\mathbf{X}}^{(t)})\| \\ & = [(\boldsymbol{\lambda}_1^{(t)} K g^{(t)} \mathbb{E}_1^{(t)})^2 + \dots + (\boldsymbol{\lambda}_I^{(t)} K g^{(t)} \mathbb{E}_I^{(t)})^2 + (\boldsymbol{\lambda}_{I+1}^{(t)} K g^{(t)} \theta_{I+1}^{(t)})^2 + \\ & \dots + (\boldsymbol{\lambda}_{2I}^{(t)} K g^{(t)} \theta_{2I}^{(t)})^2]^{\frac{1}{2}} \stackrel{18(a)}{\leq} [(K g^{(t)} \mathbb{E}_{max}^{(t)})^2 (\boldsymbol{\lambda}_1^{(t)})^2 + \dots + (\boldsymbol{\lambda}_{2I}^{(t)})^2]^{\frac{1}{2}} \\ & = [(K g^{(t)} \mathbb{E}_{max}^{(t)})^2 \|\boldsymbol{\lambda}^{(t)}\|^2]^{\frac{1}{2}} \leq \{[D^2 - (\frac{\Omega_{max}}{T})^2]^2\}^{\frac{1}{2}} \|\boldsymbol{\lambda}^{(t)}\|^{\frac{1}{2}} \\ & = [D^2 - (\frac{\Omega_{max}}{T})^2]^2 \|\boldsymbol{\lambda}^{(t)}\|, \end{aligned} \quad (18)$$

where 18(a) is due to (17). Then we can bound $\|\nabla_{\boldsymbol{\lambda}} \mathcal{L}^{(t)}(\tilde{\mathbf{X}}^{(t)}, \boldsymbol{\lambda}^{(t)})\|^2$ as follows:

$$\begin{aligned} & \|\nabla_{\boldsymbol{\lambda}} \mathcal{L}^{(t)}(\tilde{\mathbf{X}}^{(t)}, \boldsymbol{\lambda}^{(t)})\|^2 = \|\nabla_{\boldsymbol{\lambda}} f^{(t)}(\tilde{\mathbf{X}}^{(t)}) + \boldsymbol{\lambda}^{(t)} \nabla_{\boldsymbol{\lambda}} g^{(t)}(\tilde{\mathbf{X}}^{(t)})\|^2 \quad (19) \\ & \leq (\|\nabla_{\boldsymbol{\lambda}} f^{(t)}(\tilde{\mathbf{X}}^{(t)})\| + \|\boldsymbol{\lambda}^{(t)} \nabla_{\boldsymbol{\lambda}} g^{(t)}(\tilde{\mathbf{X}}^{(t)})\|)^2 \\ & \stackrel{19(a)}{\leq} \{G + [D^2 - \frac{\Omega_{max}^2}{T^2}]^2\} \|\boldsymbol{\lambda}^{(t)}\|^2 \\ & \stackrel{19(b)}{\leq} 2G^2 + 2[D^2 - \frac{\Omega_{max}^2}{T^2}]^4 \|\boldsymbol{\lambda}^{(t)}\|^2, \end{aligned}$$

where 19(a) follows assumption (1) $\|\nabla f^{(t)}(\tilde{\mathbf{X}}^{(t)})\| \leq G$ and (18). 19(b) holds by the inequality $(n_1 + n_2 + \dots + n_k)^2 \leq k(n_1^2 + n_2^2 + \dots + n_k^2)$. Next, we have $\|\nabla_{\boldsymbol{\lambda}} \mathcal{L}^{(t)}(\tilde{\mathbf{X}}^{(t)}, \boldsymbol{\lambda}^{(t)})\|^2 = \|g^{(t)}(\tilde{\mathbf{X}}^{(t)})\|^2 \leq D^2$. Then we can give the upper bound for $\frac{1}{2\alpha} \sum_{t \in \mathcal{T}} (\|\tilde{\mathbf{X}}^{(t)*} - \tilde{\mathbf{X}}^{(t)}\|^2 - \|\tilde{\mathbf{X}}^{(t)*} - \tilde{\mathbf{X}}^{(t+1)}\|^2)$ as follows:

$$\begin{aligned} & \frac{1}{2\alpha} \sum_{t=1}^T (\|\tilde{\mathbf{X}}^{(t)*} - \tilde{\mathbf{X}}^{(t)}\|^2 - \|\tilde{\mathbf{X}}^{(t)*} - \tilde{\mathbf{X}}^{(t+1)}\|^2) \quad (20) \\ & = \frac{1}{2\alpha} \sum_{t=1}^T (\|\tilde{\mathbf{X}}^{(t)} - \tilde{\mathbf{X}}^{(t+1)}\|^2) + \frac{1}{\alpha} \sum_{t=1}^T \|\tilde{\mathbf{X}}^{(t)*}\| (\|\tilde{\mathbf{X}}^{(t+1)}\| - \|\tilde{\mathbf{X}}^{(t)}\|) \\ & = \frac{1}{2\alpha} (\|\tilde{\mathbf{X}}^{(1)}\|^2 - \|\tilde{\mathbf{X}}^{(T+1)}\|^2) + \frac{1}{\alpha} \|\tilde{\mathbf{X}}^{(T+1)}\| \|\tilde{\mathbf{X}}^{(T)*}\| \\ & \quad - \frac{1}{\alpha} \|\tilde{\mathbf{X}}^{(1)}\| \|\tilde{\mathbf{X}}^{(1)*}\| \\ & \quad + \frac{1}{\alpha} \sum_{t=2}^T \|\tilde{\mathbf{X}}^{(t)}\| (\|\tilde{\mathbf{X}}^{(t-1)*}\| - \|\tilde{\mathbf{X}}^{(t)*}\|) \stackrel{20(a)}{\leq} \frac{1}{\alpha} R^2 + \frac{R}{\alpha} \mathcal{V}_{\tilde{\mathbf{X}}^{(t)*}}^T, \end{aligned}$$

where 20(a) follows assumption (2) and the accumulated hindsight optimum variation $\mathcal{V}_{\tilde{\mathbf{X}}^{(t)*}}^T = \sum_{t=2}^T (\|\tilde{\mathbf{X}}^{(t-1)*} - \tilde{\mathbf{X}}^{(t)*}\|)$. Next is to upper bound $\frac{1}{2\mu} \sum_{t=1}^T (\|\boldsymbol{\lambda} - \boldsymbol{\lambda}^{(t)}\|^2 - \|\boldsymbol{\lambda} - \boldsymbol{\lambda}^{(t+1)}\|^2)$.

$$\begin{aligned} & \frac{1}{2\mu} \sum_{t=1}^T (\|\boldsymbol{\lambda} - \boldsymbol{\lambda}^{(t)}\|^2 - \|\boldsymbol{\lambda} - \boldsymbol{\lambda}^{(t+1)}\|^2) \leq \\ & \quad \frac{1}{2\mu} (\|\boldsymbol{\lambda} - \boldsymbol{\lambda}^{(1)}\|^2 - \|\boldsymbol{\lambda} - \boldsymbol{\lambda}^{(T+1)}\|^2) \stackrel{21(a)}{\leq} \frac{1}{2\mu} \|\boldsymbol{\lambda}\|^2, \end{aligned} \quad (21)$$

where 21(a) is due to $\boldsymbol{\lambda}^{(1)} = 0$ and $\boldsymbol{\lambda}^{(T+1)} \geq \boldsymbol{\lambda}$, which is decided by its non-negativity. Finally, based on the above, we can expand Lemma 3 over the entire time horizon as follows:

$$\begin{aligned} & \sum_t \mathcal{L}(\tilde{\mathbf{X}}_t, \boldsymbol{\lambda}) - \sum_t \mathcal{L}(\tilde{\mathbf{X}}_t^*, \boldsymbol{\lambda}_t) \\ & \leq \sum_t \nabla_{\boldsymbol{\lambda}} \mathcal{L}(\tilde{\mathbf{X}}_t, \boldsymbol{\lambda}_t) (\tilde{\mathbf{X}}_t - \tilde{\mathbf{X}}_t^*) - \sum_t \nabla_{\boldsymbol{\lambda}} \mathcal{L}(\tilde{\mathbf{X}}_t, \boldsymbol{\lambda}_t) (\boldsymbol{\lambda} - \boldsymbol{\lambda}_t) \\ & \leq \frac{1}{2\alpha} \sum_{t \in \mathcal{T}} (\|\tilde{\mathbf{X}}_t^* - \tilde{\mathbf{X}}_t\|^2 - \|\tilde{\mathbf{X}}_t^* - \tilde{\mathbf{X}}_{t+1}\|^2) + \frac{\mu}{2} \sum_{t \in \mathcal{T}} \|\nabla_{\boldsymbol{\lambda}} \mathcal{L}(\tilde{\mathbf{X}}_t, \boldsymbol{\lambda}_t)\|^2 \\ & \quad + \frac{\alpha}{2} \sum_{t \in \mathcal{T}} \|\nabla_{\boldsymbol{\lambda}} \mathcal{L}(\tilde{\mathbf{X}}_t, \boldsymbol{\lambda}_t)\|^2 + \frac{1}{2\mu} \sum_{t \in \mathcal{T}} (\|\boldsymbol{\lambda} - \boldsymbol{\lambda}_t\|^2 - \|\boldsymbol{\lambda} - \boldsymbol{\lambda}_{t+1}\|^2) \\ & = \frac{R^2 + R\mathcal{V}_{\tilde{\mathbf{X}}^{(t)*}}^T}{\alpha} + \frac{\|\boldsymbol{\lambda}\|^2}{2\mu} + \frac{T\mu D^2}{2} + 2\alpha G^2 T \\ & \quad + 2\alpha [D^2 - (\frac{\Omega_{max}}{T})^2]^4 \mathcal{V}_{\boldsymbol{\lambda}^{(t)}}^T. \end{aligned}$$

□

B. Proof of Theorem 2

Having the above three supporting lemmas, we can prove Theorem 2 as follows:

$$\begin{aligned} & \sum_{t \in \mathcal{T}} \left[f(\tilde{\mathbf{X}}^{(t)}) - f(\tilde{\mathbf{X}}^{(t)*}) \right] + \sum_{t \in \mathcal{T}} \left[\boldsymbol{\lambda}^\top g(\tilde{\mathbf{X}}^{(t)}) - \boldsymbol{\lambda}^{(t)} g(\tilde{\mathbf{X}}^{(t)*}) \right] \\ & \leq \frac{R^2 + R\mathcal{V}_{\tilde{\mathbf{X}}^{(t)*}}^T}{\alpha} + \frac{\|\boldsymbol{\lambda}\|^2 / \mu + T\mu D^2}{2} \\ & + 2\alpha G^2 T + 2\alpha[D^2 - (\frac{\Omega_{max}}{T})^2]^4 \mathcal{V}_{\boldsymbol{\lambda}^{(t)}}^T. \end{aligned}$$

Due to $\sum_{t \in \mathcal{T}} \boldsymbol{\lambda}^{(t)} g(\tilde{\mathbf{X}}^{(t)*}) \geq 0$, we can get

$$\begin{aligned} & \frac{R^2 + R\mathcal{V}_{\tilde{\mathbf{X}}^{(t)*}}^T}{\alpha} + \frac{T\mu D^2}{2} + 2\alpha G^2 T + 2\alpha[D^2 - (\frac{\Omega_{max}}{T})^2]^4 \mathcal{V}_{\boldsymbol{\lambda}^{(t)}}^T \\ & \geq \sum_{t \in \mathcal{T}} f^{(t)}(\tilde{\mathbf{X}}^{(t)}) - \sum_{t \in \mathcal{T}} f^{(t)}(\tilde{\mathbf{X}}^{(t)*}) + \sum_{t \in \mathcal{T}} \boldsymbol{\lambda}^\top g^{(t)}(\tilde{\mathbf{X}}^{(t)}) - \frac{\|\boldsymbol{\lambda}\|^2}{2\mu} \\ & \stackrel{22(a)}{\geq} \sum_{t \in \mathcal{T}} f^{(t)}(\tilde{\mathbf{X}}^{(t)}) - \sum_{t \in \mathcal{T}} f^{(t)}(\tilde{\mathbf{X}}^{(t)*}) + \frac{\mu g^{(t)}(\tilde{\mathbf{X}}^{(t)})}{2} \\ & \geq \sum_{t \in \mathcal{T}} f^{(t)}(\tilde{\mathbf{X}}^{(t)}) - \sum_{t \in \mathcal{T}} f^{(t)}(\tilde{\mathbf{X}}^{(t)*}) = \widetilde{D}_{\text{fit}}^{(T)}, \end{aligned} \quad (22)$$

where 22(a) is due to $\sum_{t \in \mathcal{T}} \boldsymbol{\lambda}^\top g^{(t)}(\tilde{\mathbf{X}}^{(t)}) - \frac{\|\boldsymbol{\lambda}\|^2}{2\mu} \leq \frac{\mu g^{(t)}(\tilde{\mathbf{X}}^{(t)})}{2}$, when $\|\boldsymbol{\lambda}\| = \mu g^{(t)}(\tilde{\mathbf{X}}^{(t)})$. As for the upper bound of dynamic fit, according to the dual recursion in Algorithm 2 and the proof of $\|\boldsymbol{\lambda}^{(t)}\| \leq \|\bar{\boldsymbol{\lambda}}\|$ in [6] Lemma 2, we have: $[\boldsymbol{\lambda}^{(T)} + \mu g^{(T)}(\tilde{\mathbf{X}}^{(T)})]^\top \geq \dots \geq \boldsymbol{\lambda}^{(1)} + \sum_{t=1}^T \mu g^{(t)}(\tilde{\mathbf{X}}^{(t)})$. Then we can rearrange the items, and then obtain $\sum_{t=1}^T g^{(t)}(\tilde{\mathbf{X}}^{(t)}) \leq \frac{\boldsymbol{\lambda}^{(T+1)}}{\mu} - \frac{\boldsymbol{\lambda}^{(1)}}{\mu} \leq \frac{\boldsymbol{\lambda}^{(T+1)}}{\mu}$. Therefore, $\widetilde{D}_{\text{fit}}^{(T)} = \left\| \sum_{t=1}^T g^{(t)}(\tilde{\mathbf{X}}^{(t)}) \right\| \leq \left\| \frac{\boldsymbol{\lambda}^{(T+1)}}{\mu} \right\| \leq \frac{\|\bar{\boldsymbol{\lambda}}\|}{\mu}$.

C. Proof of Theorem 3

(1) For proving that $E(\bar{x}_i^{(t)})$ is monotonically non-increasing in $c_i^{(t)}$. We first let $\mathbf{C}(\bar{x}_i^{(t)}, c_i^{(t)}, \mathbf{c}_{-i}^{(t)})$ denotes the objective value of the problem in (3) with reported prices $(c_i^{(t)}, \mathbf{c}_{-i}^{(t)})$, where $c_i^{(t)}$ denotes the bidding price of vehicle i and $\mathbf{c}_{-i}^{(t)}$ denotes all the other prices except i . We fix $\mathbf{c}_{-i}^{(t)}$ and define $\tilde{x}_i^{(t)}$ and $\bar{x}_i^{(t)}$ as the optimal fractional results of i with bid $c_i^{(t)}$ and $\bar{c}_i^{(t)}$. In the case that $c_i^{(t)} \geq \bar{c}_i^{(t)}$, we have

$$\begin{aligned} \mathbf{C}(\tilde{x}_i^{(t)}, c_i^{(t)}, \mathbf{c}_{-i}^{(t)}) & \leq \mathbf{C}(\bar{x}_i^{(t)}, c_i^{(t)}, \mathbf{c}_{-i}^{(t)}) \\ \mathbf{C}(\tilde{x}_i^{(t)}, \bar{c}_i^{(t)}, \mathbf{c}_{-i}^{(t)}) & \leq \mathbf{C}(\bar{x}_i^{(t)}, \bar{c}_i^{(t)}, \mathbf{c}_{-i}^{(t)}). \end{aligned}$$

After adding the above inequalities together and reformulate them, we can obtain

$$\begin{aligned} (c_i^{(t)} - \bar{c}_i^{(t)}) \cdot \tilde{x}_i^{(t)} & \leq (c_i^{(t)} - \bar{c}_i^{(t)}) \cdot \bar{x}_i^{(t)} \\ \Rightarrow \bar{x}_i^{(t)} & \leq \tilde{x}_i^{(t)}, \Rightarrow E(\bar{x}_i^{(t)}) \leq E(\tilde{x}_i^{(t)}). \end{aligned}$$

(2) We denote $\varkappa_i^{(t)}$ as the upper bound of the integral of $\int_0^\infty E(\bar{x}_i^{(t)}) dc < \infty$, which is due to an extreme case: when the cost of vehicle i is larger than the cost of self-training at server, $\varkappa_i^{(t)} = \mathcal{V} \log_2(\frac{1}{\theta_i^{(t)}}) M \zeta_1^{(t)} + |D_i^{(t)}| \zeta_2^{(t)}$, then we have

$$\begin{aligned} & \int_0^\infty E(\bar{x}_i^{(t)}(c, \mathbf{c}_{-i}^{(t)})) dc = \int_0^{\varkappa_i^{(t)}} E(\bar{x}_i^{(t)}(c, \mathbf{c}_{-i}^{(t)})) dc \\ & = \int_0^{\mathcal{V} \log_2(\frac{1}{\theta_i^{(t)}}) M \zeta_1^{(t)} + |D_i^{(t)}| \zeta_2^{(t)}} \bar{x}_i^{(t)}(c, \mathbf{c}_{-i}^{(t)}) dc \\ & \leq \mathcal{V} \log_2(\frac{1}{\theta_i^{(t)}}) M \zeta_1^{(t)} + |D_i^{(t)}| \zeta_2^{(t)} < \infty. \end{aligned}$$

(3) As for individual rationality in expectation, we have

$$\begin{aligned} r_i^{(t)} & = c_i^{(t)} E(\bar{x}_i^{(t)}(c, \mathbf{c}_{-i}^{(t)})) + \int_{c_i^{(t)}}^{\varkappa_i^{(t)}} E(\bar{x}_i^{(t)}(c, \mathbf{c}_{-i}^{(t)})) dc, \\ u_i^{(t)} & = r_i^{(t)} - c_i^{(t)} E(\bar{x}_i^{(t)}(c, \mathbf{c}_{-i}^{(t)})) = \int_{c_i^{(t)}}^{\varkappa_i^{(t)}} E(\bar{x}_i^{(t)}(c, \mathbf{c}_{-i}^{(t)})) dc \geq 0. \end{aligned}$$

REFERENCES

- [1] Z. Yang, M. Chen, W. Saad, C. S. Hong, and M. Shikh-Bahaei, “Energy efficient federated learning over wireless communication networks,” *IEEE Transactions on Wireless Communications*, vol. 20, no. 3, pp. 1935–1949, 2021.
- [2] S. Wang, T. Tuor, T. Salonidis, K. K. Leung, C. Makaya, T. He, and K. Chan, “Adaptive federated learning in resource constrained edge computing systems,” *IEEE Journal on Selected Areas in Communications*, vol. 37, no. 6, pp. 1205–1221, 2019.
- [3] Y. Lu, X. Huang, Y. Dai, S. Maharjan, and Y. Zhang, “Federated learning for data privacy preservation in vehicular cyber-physical systems,” *IEEE Network*, vol. 34, no. 3, pp. 50–56, 2020.
- [4] D. Ye, R. Yu, M. Pan, and Z. Han, “Federated learning in vehicular edge computing: A selective model aggregation approach,” *IEEE Access*, vol. 8, pp. 23920–23935, 2020.
- [5] H. Yu, Z. Liu, Y. Liu, T. Chen, M. Cong, X. Weng, D. Niyato, and Q. Yang, “A sustainable incentive scheme for federated learning,” *IEEE Intelligent Systems*, vol. 35, no. 4, pp. 58–69, 2020.
- [6] Y. Jin, L. Jiao, Z. Qian, S. Zhang, S. Lu, and X. Wang, “Resource-efficient and convergence-preserving online participant selection in federated learning,” in *IEEE International Conference on Distributed Computing Systems (ICDCS)*, 2020.
- [7] Y. Chen, S. He, F. Hou, Z. Shi, and J. Chen, “An efficient incentive mechanism for device-to-device multicast communication in cellular networks,” *IEEE Transactions on Wireless Communications*, vol. 17, no. 12, pp. 7922–7935, 2018.
- [8] Y. Zhan and J. Zhang, “An incentive mechanism design for efficient edge learning by deep reinforcement learning approach,” in *IEEE International Conference on Computer Communications (INFOCOM)*, 2020.
- [9] S. R. Pandey, N. H. Tran, M. N. H. Tran, A. Manzoor, and C. S. Hong, “A crowdsourcing framework for on-device federated learning,” *IEEE Transactions on Wireless Communications*, vol. 19, no. 5, pp. 3241–3256, 2020.
- [10] T. H. T. Le, N. H. Tran, Y. K. Tun, M. N. H. Nguyen, S. R. Pandey, Z. Han, and C. S. Hong, “An incentive mechanism for federated learning in wireless cellular network: An auction approach,” *IEEE Transactions on Wireless Communications*, pp. 1–1, 2021.
- [11] S. Chen, Z. Zhou, F. Liu, Z. Li, and S. Ren, “Cloudheat: An efficient online market mechanism for datacenter heat harvesting,” *ACM Transactions on Modeling and Performance Evaluation of Computing Systems*, vol. 3, no. 3, pp. 11:1–11:31, 2018.
- [12] R. Zeng, S. Zhang, J. Wang, and X. Chu, “Fmore: An incentive scheme of multi-dimensional auction for federated learning in m2c,” in *2020 IEEE 40th International Conference on Distributed Computing Systems (ICDCS)*, 2020, pp. 278–288.
- [13] J. Konecný, H. B. McMahan, D. Ramage, and P. Richtárik, “Federated optimization: Distributed machine learning for on-device intelligence,” *CoRR*, vol. abs/1610.02527, 2016.
- [14] Y. M. Saputra, D. T. Hoang, D. N. H. Nguyen, E. Dutkiewicz, M. D. Mueck, and S. Srikantewara, “Energy demand prediction with federated learning for electric vehicle networks,” in *IEEE Global Communications Conference (GLOBECOM)*, 2019.
- [15] N. H. Tran, W. Bao, A. Zomaya, M. N. H. Nguyen, and C. S. Hong, “Federated learning over wireless networks: Optimization model design and analysis,” in *IEEE International Conference on Computer Communications (INFOCOM)*, 2019.
- [16] M. Chen, Z. Yang, W. Saad, C. Yin, H. V. Poor, and S. Cui, “A joint learning and communications framework for federated learning over wireless networks,” *IEEE Transactions on Wireless Communications*, vol. 20, no. 1, pp. 269–283, 2021.
- [17] H. T. Nguyen, V. Sehwag, S. Hosseinalipour, C. G. Brinton, M. Chiang, and H. Vincent Poor, “Fast-convergent federated learning,” *IEEE Journal on Selected Areas in Communications*, vol. 39, no. 1, pp. 201–218, 2021.
- [18] H. Wang, Z. Kaplan, D. Niu, and B. Li, “Optimizing federated learning on non-iid data with reinforcement learning,” in *IEEE International Conference on Computer Communications (INFOCOM)*, 2020.

- [19] J. Kang, Z. Xiong, D. Niyato, S. Xie, and J. Zhang, "Incentive mechanism for reliable federated learning: A joint optimization approach to combining reputation and contract theory," *IEEE Internet of Things Journal*, vol. 6, no. 6, pp. 10700–10714, 2019.
- [20] Y. Jiao, P. Wang, D. Niyato, B. Lin, and D. I. Kim, "Toward an automated auction framework for wireless federated learning services market," *IEEE Transactions on Mobile Computing*, pp. 1–1, 2020.
- [21] E. C. Hall and R. M. Willett, "Online convex optimization in dynamic environments," *IEEE Journal of Selected Topics in Signal Processing*, vol. 9, no. 4, pp. 647–662, 2015.
- [22] T. Chen, Q. Ling, and G. B. Giannakis, "An online convex optimization approach to proactive network resource allocation," *IEEE Transactions on Signal Processing*, vol. 65, no. 24, pp. 6350–6364, 2017.
- [23] R. D. Carr, L. K. Fleischer, V. J. Leung, and C. A. Phillips, "Strengthening integrality gaps for capacitated network design and covering problems," in *ACM-SIAM Symposium on Discrete Algorithms (SODA)*, 2000.
- [24] Z. Wang, B. Kim, and L. P. Kaelbling, "Regret bounds for meta bayesian optimization with an unknown gaussian process prior," in *Advances in Neural Information Processing Systems (NIPS)*, 2018.
- [25] T. Chen, Q. Ling, Y. Shen, and G. B. Giannakis, "Heterogeneous online learning for a thing-adaptive fog computing in iot," *IEEE Internet of Things Journal*, vol. 5, no. 6, pp. 4328–4341, 2018.
- [26] S. Feng, D. Niyato, P. Wang, D. I. Kim, and Y. Liang, "Joint service pricing and cooperative relay communication for federated learning," in *International Conference on Internet of Things (iThings) and IEEE Green Computing and Communications (GreenCom) and IEEE Cyber, Physical and Social Computing (CPSCom) and IEEE Smart Data (SmartData)*, 2019.
- [27] Y. Zhan, P. Li, Z. Qu, D. Zeng, and S. Guo, "A learning-based incentive mechanism for federated learning," *IEEE Internet of Things Journal*, vol. 7, no. 7, pp. 6360–6368, 2020.
- [28] N. Ding, Z. Fang, and J. Huang, "Optimal contract design for efficient federated learning with multi-dimensional private information," *IEEE Journal on Selected Areas in Communications*, vol. 39, no. 1, pp. 186–200, 2021.
- [29] J. Mills, J. Hu, and G. Min, "Communication-efficient federated learning for wireless edge intelligence in iot," *IEEE Internet of Things Journal*, vol. 7, no. 7, pp. 5986–5994, 2020.
- [30] Z. Zhou, S. Yang, L. Pu, and S. Yu, "Cefl: Online admission control, data scheduling, and accuracy tuning for cost-efficient federated learning across edge nodes," *IEEE Internet of Things Journal*, vol. 7, no. 10, pp. 9341–9356, 2020.
- [31] L. Wang, W. Wang, and B. Li, "Cmfl: Mitigating communication overhead for federated learning," in *IEEE International Conference on Distributed Computing Systems (ICDCS)*, 2019.
- [32] L. Li, J. Wang, X. Chen, and C. Z. Xu, "Multi-layer coordination for high-performance energy-efficient federated learning," in *IEEE/ACM International Symposium on Quality of Service (IWQoS)*, 2020.
- [33] C. T. Dinh, N. H. Tran, M. N. H. Nguyen, C. S. Hong, W. Bao, A. Y. Zomaya, and V. Gramoli, "Federated learning over wireless networks: Convergence analysis and resource allocation," *IEEE/ACM Transactions on Networking*, pp. 1–12, 2020.
- [34] D. Liu and O. Simeone, "Privacy for free: Wireless federated learning via uncoded transmission with adaptive power control," *IEEE Journal on Selected Areas in Communications*, vol. 39, no. 1, pp. 170–185, 2021.
- [35] S. Prakash, S. Dhakal, M. R. Akdeniz, Y. Yona, S. Talwar, S. Avestimehr, and N. Himayat, "Coded computing for low-latency federated learning over wireless edge networks," *IEEE Journal on Selected Areas in Communications*, vol. 39, no. 1, pp. 233–250, 2021.
- [36] S. Mizuno and F. Jarre, "Global and polynomial-time convergence of an infeasible-interior-point algorithm using inexact computation," *Mathematical Programming*, vol. 84, no. 1, 1999.
- [37] X. Gao, M. Sitharam, and A. E. Roitberg, "Bounds on the jensen gap, and implications for mean-concentrated distributions," *The Australian Journal of Mathematical Analysis and Applications*, vol. 16, no. 2, pp. 1–16, 2019.
- [38] A. Archer and É. Tardos, "Truthful mechanisms for one-parameter agents," in *IEEE Symposium on Foundations of Computer Science (FOCS)*, 2001.
- [39] Y. Lecun, L. Bottou, Y. Bengio, and P. Haffner, "Gradient-based learning applied to document recognition," *Proceedings of the IEEE*, vol. 86, no. 11, pp. 2278–2324, 1998.
- [40] H. Xiao, K. Rasul, and R. Vollgraf, "Fashion-mnist: a novel image dataset for benchmarking machine learning algorithms," *CoRR*, vol. abs/1708.07747, 2017.
- [41] "Pytorch," <https://pytorch.org/>.
- [42] H. B. McMahan, E. Moore, D. Ramage, S. Hampson, and B. A. y. Arcas, "Communication-efficient learning of deep networks from decentralized data," 2016.
- [43] T. Li, A. K. Sahu, M. Zaheer, M. Sanjabi, A. Talwalkar, and V. Smith, "Federated optimization in heterogeneous networks," in *The Conference on Machine Learning and Systems (MLSys)*, 2020.
- [44] S. Zaman and D. Grosu, "Combinatorial auction-based allocation of virtual machine instances in clouds," in *2010 IEEE Second International Conference on Cloud Computing Technology and Science*, 2010, pp. 127–134.
- [45] "Build efficient optimal control software, with minimal effort." <https://web.casadi.org/>.



Yulan Yuan received the BEng degree in Telecommunications Engineering with Management from Beijing University of Posts and Telecommunications, China, in 2019. She is now a master student in School of Artificial Intelligence in Beijing University of Posts and Telecommunications. Her research interests are in the areas of distributed computing, intelligent transportation, and federated learning.



Lei Jiao received the Ph.D. degree in computer science from the University of Göttingen, Germany. He is currently an assistant professor at the Department of Computer and Information Science, University of Oregon, USA. Previously he worked as a member of technical staff at Alcatel-Lucent/Nokia Bell Labs in Dublin, Ireland and also as a researcher at IBM Research in Beijing, China. He is interested in the mathematics of optimization, control, learning, and mechanism design, applied to computer and telecommunication systems, networks, and services.

He publishes papers in journals such as IEEE/ACM Transactions on Networking, IEEE Transactions on Parallel and Distributed Systems, IEEE Transactions on Mobile Computing, and IEEE Journal on Selected Areas in Communications, and in conferences such as INFOCOM, MOBIHOC, ICNP, and ICDCS. He is a recipient of the NSF CAREER Award. He also received the Best Paper Awards of IEEE LANMAN 2013 and IEEE CNS 2019, and the 2016 Alcatel-Lucent Bell Labs UK and Ireland Recognition Award. He served as a guest editor for IEEE JSAC. He was on the program committees of conferences including INFOCOM, MOBIHOC, ICDCS, and IWQoS, and was also the program chair of multiple workshops with INFOCOM and ICDCS.



Konglin Zhu received the master's degree in computer Science from the University of California, Los Angeles, CA, USA, and the Ph.D. degree from the University of Göttingen, Germany, in 2009 and 2014, respectively. He is now an Associate Professor with the Beijing University of Posts and Telecommunications, Beijing, China. His research interests include Internet of Vehicles and V2X communications.



Lin Zhang received the B.S. and the Ph.D. degrees in 1996 and 2001, both from the Beijing University of Posts and Telecommunications, Beijing, China. From 2000 to 2004, he was a Postdoctoral Researcher with Information and Communications University, Daejeon, South Korea, and Nanyang Technological University, Singapore, respectively. He joined Beijing University of Posts and Telecommunications in 2004, where he has been a Professor since 2011. His current research interests include mobile cloud computing and Internet of Things.